

UNIVERSITY OF GHANA

COLLEGE OF BASIC AND APPLIED SCIENCES

**DEPENDENCE OF TELETHERAPY TIMER ERROR ON TREATMENT
PARAMETERS IN EXTERNAL BEAM RADIOTHERAPY (EBRT) USING THE
THERATRON EQUINOX 100 COBALT 60 MACHINE**

BY

NANA KOREE BOAKYE

(10508448)

**THIS THESIS IS SUBMITTED TO THE UNIVERSITY OF GHANA, LEGON IN
PARTIAL FULFILLMENT OF THE REQUIREMENT FOR THE AWARD OF
MPHIL MEDICAL PHYSICS DEGREE**

**DEPARTMENT OF MEDICAL PHYSICS, SCHOOL OF NUCLEAR AND
ALLIED SCIENCES**

JULY, 2016

DECLARATION

This thesis is the result of research work undertaken by Nana Koree Boakye in the Department of Medical Physics, School of Nuclear and Allied Sciences, University of Ghana, under the supervision of Prof. Cyril Schandorf, Dr. Francis Hasford and Mr. Samuel N. A. Tagoe.

It is my conviction that, no part of this work has been presented in part or whole to any other university or institution for the award of a diploma, or degree at any level. Related works and research work done cited in this work have been acknowledged under references.

.....
NANA KOREE BOAKYE

(STUDENT)

Date.....

.....
PROF. CYRIL SCHANDORF

(PRINCIPAL SUPERVISOR)

Date.....

.....
DR. FRANCIS HASFORD

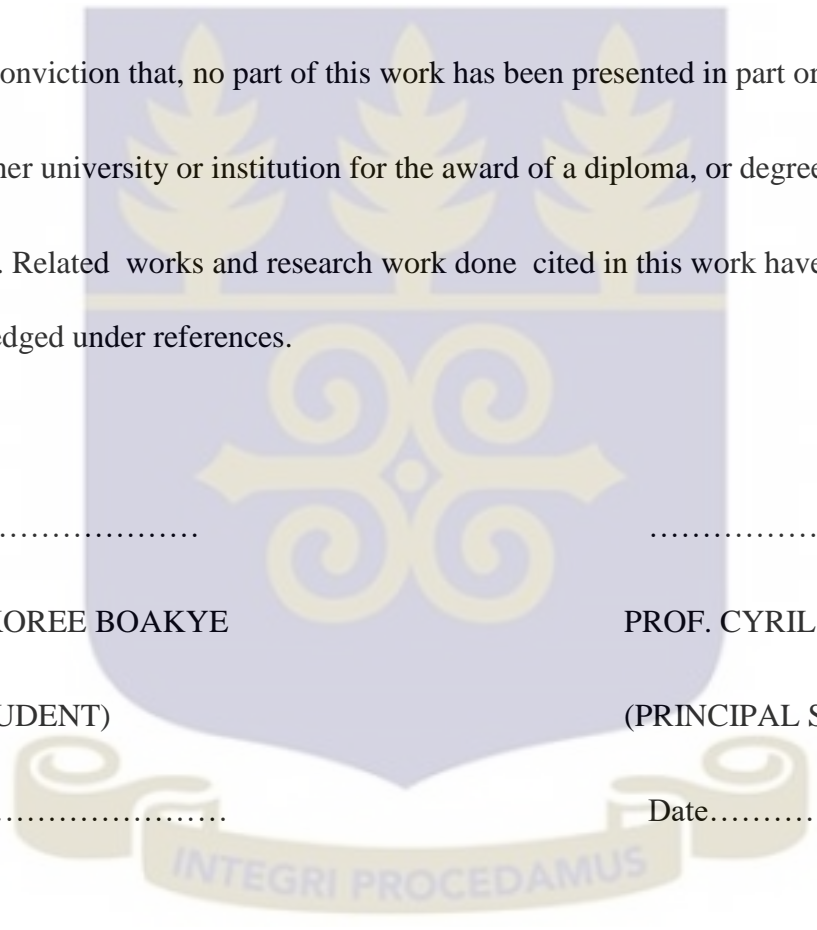
(CO-SUPERVISOR)

Date.....

.....
MR. SAMUEL N. A. TAGOE

(CO-SUPERVISOR)

Date.....



ABSTRACT

The purpose of this research work is to evaluate the variation (or dependence) of the timer error as a function of the teletherapy treatment parameters such as treatment field size (FS) and treatment depth (d) for a SSD setup and compare the method used for others. Teletherapy timer error measurements were performed in a full scatter, large water phantom using a 0.6cc ionization chamber and an average photon energy of 1.25MeV from a cobalt-60 unit at an SSD of 100cm at various field size variations and treatment depth variation with gantry and collimator angles fixed at 0°. From the measurements taken, the timer error for the treatment field size variations of $5\times 5\text{cm}^2$, $10\times 10\text{cm}^2$, $15\times 15\text{cm}^2$, $20\times 20\text{cm}^2$, $30\times 30\text{cm}^2$, $35\times 35\text{cm}^2$ were found to be 0.654s, 0.648s, 0.622s, 0.633s, 0.639s and 0.643s respectively for a constant depth of 5cm; and the timer error for treatment depth variations of 5cm, 7cm, 10cm, 15cm and 20cm were found to be 0.648s, 0.585s, 0.612s, 0.665s and 0.6215s for a constant field size of $10\times 10\text{cm}^2$. Comparing the two set-up techniques used with this work, it was noted that the field size variation and depth variation showed almost similar timer value to the order of 10^{-1} . However, the treatment depth variations showed the lowest value as compared to treatment depths. The treatment depth of 15cm recorded the highest timer error of 0.665s and the treatment depth of 7cm showed the lowest value of the timer error of 0.585s. The timer error calculated for this experimental work with the variations in field size was found to vary in the range of 26.47% to 30.13% to the last teletherapy timer error value of 0.89s. The timer error for the variations in treatment depth was found to vary in the range of 25.27% to 34.31% to the last teletherapy timer error value of 0.89s. The conclusion of this work is that timer error depends on both field size and treatment

depth and must be taken into account by the creation of a Lookup Table similar to Tissue maximum ratio (TMR) and Tissue Phantom ratio (TPR) Tables to account for these variations during treatment planning and /or manual dose calculations.



DEDICATION

This work is dedicated to my parents Mr. and Mrs. Boakye, my siblings and to all my loved ones.



ACKNOWLEDGMENTS

My first and foremost thanks and appreciation goes to God Almighty for his protection and guidance for me, giving me the sound health, wisdom, knowledge and providing me with what I needed to pursue this research work.

I wish to express thanks and appreciation to my supervisor Prof. Cyril Schandoff, Dr Francis Hasford and Mr Samuel Nii Adu Tagoe for their positivity toward the work and encouragements through the work. I am deeply grateful for his guidance and support.

I also recognize and thank all the staff of the Medical Physics Unit especially Mr Evans Sasu of the National Centre of Radiotherapy and Nuclear Medicine, Korle Bu for their cooperation and time spent with support through the experimental process of this work.

I am indebted to the Medical Physics department especially Prof. K. W. E.. Kyere for his candid and open discussions. The technical and administrative support received from you throughout my MPhil. Program is highly acknowledged.

I am most grateful to my parents Mr. and Mrs. Boakye and my siblings Nana Ama Boakye, Paa Joe Boakye, Maataa Safoa Boakye and Ataaku Safo Boakye and my dearest Lily Aba Crentsil for being great impacts through love, emphatic encouragement and prayers which has made this work possible.

TABLE OF CONTENTS

DECLARATION	i
ABSTRACT.....	ii
DEDICATION	iv
ACKNOWLEDGMENTS.....	v
TABLE OF CONTENTS.....	vi
LIST OF FIGURES.....	ix
LIST OF TABLES.....	xi
LIST OF ABBREVIATIONS	xii
CHAPTER ONE	1
INTRODUCTION.....	1
1.1 BACKGROUND.....	1
1.2 STATEMENT OF THE PROBLEM	3
1.3 OBJECTIVES	4
1.4 RELEVANCE AND JUSTIFICATION	5
1.5 SCOPE OF STUDY.....	5
1.6 ARRANGEMENT OF THE THESIS	6
CHAPTER TWO	7
2.1 INTRODUCTION.....	7
2.2 THE COBALT-60 MACHINE	7
2.2.1 Background	7
2.2.2 Basic Construction and Components.....	9
2.2.3 Beam modifiers.....	13
2.3 OUTPUT FACTORS	14
2.4 Collimator system	15

2.5 Treatment Parameters.....	16
2.6 Source to surface distance (SSD) and Source to axis distance (SAD).....	16
2.7 Field Size	18
2.8 EFFECTS AND REVIEW OF TIMER ERROR	19
CHAPTER THREE	22
MATERIALS AND METHODS.....	22
3.1 MATERIALS.....	22
3.1.1 Theratron Equinox 100 Co-60 teletherapy unit.....	23
3.1.2 Farmer type ionization chamber.....	24
3.1.3 PTW UNIDOS Electrometer.....	25
3.1.4 2-Dimensional Water phantom	26
3.1.5 SOFTWARE	27
3.2 METHOD.....	28
3.2.1 Stability check	28
3.2.2 General Procedure and Experimental Setup	28
3.3 DATA ANALYSIS	34
3.3.1 CALCULATIONS AND GRAPH PLOTTING.....	34
CHAPTER FOUR	37
RESULTS AND DISCUSSION	37
4.1 INTRODUCTION.....	37
4.2 DEPENDENCE ON FIELD SIZE	37
4.3 DEPENDENCE ON TREATMENT DEPTH	42
CHAPTER FIVE	48
CONCLUSION AND RECOMMENDATION	48
5.1 CONCLUSION.....	48
5.2 RECOMMENDATION	49
5.2.1 Clinical Community	49
5.2.2 Policy Makers and Regulators.....	50
5.2.3 Research community	50

REFERENCES..... 51

APPENDICES..... 57



LIST OF FIGURES

	PAGE
Figure 2.1: A diagram showing inside the head of a teletherapy gantry	10
Figure 2.2: Schematic diagram of the SSD or SAD setups which may be used for photon beam reference dosimetry for equivalent depth.	18
Fig 3.1(a): Digital thermometer	23
Fig 3.1(b): Barometer	23
Fig 3.2: The Theratron Equinox 100 Cobalt 60 machine at Korle Bu	24
Figure 3.3: Farmer type ionization chamber.	25
Figure 3.4: The PTW UNIDOS electrometer	26
Figure 3.5: Large water phantom	27
Fig 3.6: Laser setup during experimental work	29
Fig 3.7: General experimental Setup	30
Fig 3.8: Treatment Control Console	30
Fig 3.9: Chamber holder used during this experiment	31
Figure 4.1: A graph of corrected electrometer reading against treatment time for a $5 \times 5 \text{ cm}^2$ field size	38

Figure 4.2: A graph of corrected electrometer reading against treatment
time for a $10 \times 10 \text{ cm}^2$ field size 39

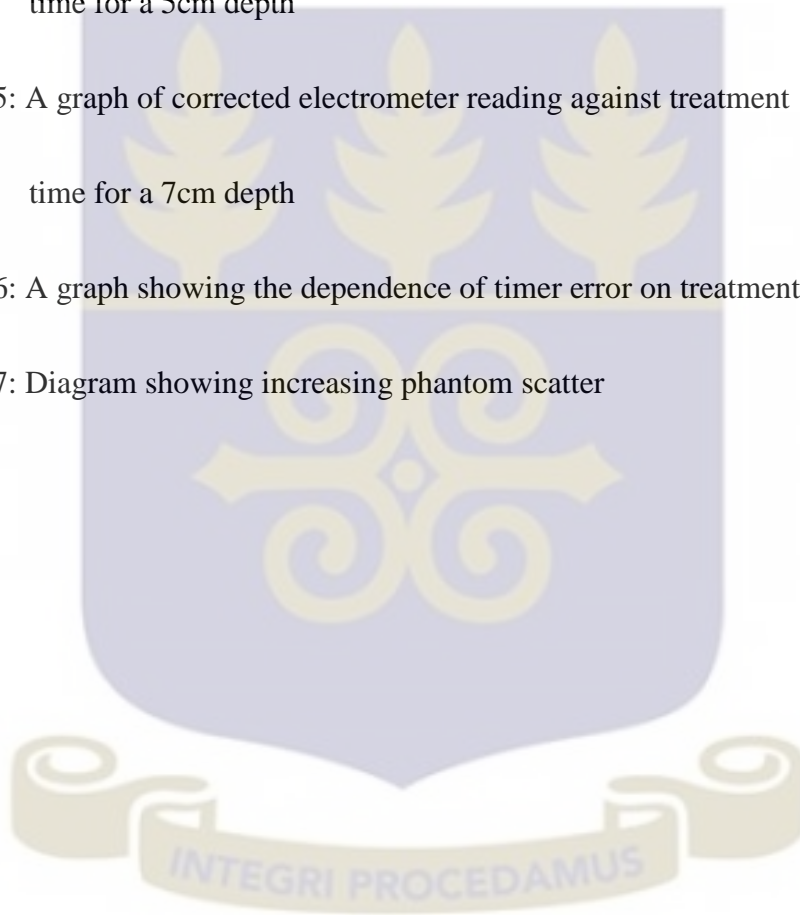
Figure 4.3: A graph showing the dependence of timer error on field size 41

Figure 4.4: A graph of corrected electrometer reading against treatment
time for a 5cm depth 43

Figure 4.5: A graph of corrected electrometer reading against treatment
time for a 7cm depth 43

Figure 4.6: A graph showing the dependence of timer error on treatment depth 45

Figure 4.7: Diagram showing increasing phantom scatter 46



LIST OF TABLES

	PAGE
Table 4.1: Field size with timer errors obtained for their setup	39
Table 4.2: Treatment depth with timer errors obtained for their setup	44



LIST OF ABBREVIATIONS

RT	Radiation therapy/Radiotherapy
EBRT	External Beam Radiation Therapy
Co-60	Cobalt 60
NCRNM	National Center of Radiotherapy and Nuclear Medicine
KBTH	Korle Bu Teaching Hospital
LINACs	Linear Accelerators
TF	Transmission Factor
FS	Field size
d	Treatment depth
SAD	Source to Axis Distance
SSD	Source to Surface Distance
d _{max}	Depth of maximum dose (0.5cm for cobalt)
ISL	Inverse Square Law
MUs	Monitor units
TMR	Tissue maximum ratio
TPR	Tissue Phantom ratio
Sc _p	Scatter factor
Sc	Collimator scatter factor
Sp	Phantom scatter factor

CHAPTER ONE

INTRODUCTION

1.1 BACKGROUND

Radiation therapy (radiotherapy) is the medical use of ionizing radiation in the treatment or control of cancer. There are other ways of treating cancer but radiotherapy is known to be used to manage “two thirds” of cancer patients worldwide [1]. Radiotherapy is also known to be used alone in the treatment or used side by side with other treatment modalities like surgery, chemotherapy or immunotherapy. When it is used before surgery the purpose is to shrink the tumor before removal, if used after surgery its goal is to destroy residual tumor or tumor left behind after surgery [1,2]. Radiotherapy can be divided into two main treatment types being external beam radiation treatment (teletherapy) and localized radiation treatment (brachytherapy). Teletherapy is known to be a type of radiation therapy with the source at a distance from the body or treatment area while brachytherapy is delivered by placing the source surgically into the tumor or by the use of catheters or seeds directly into or near to the tumor. For teletherapy, the dose is inversely proportional to the distance. In brachytherapy, dose fall-off from the centre of the source is very high due to the inverse square law effect, and hence normal surrounding tissues are spared from excessive radiation [3].

Teletherapy began soon after Wilhelm Röntgen’s discovery of X ray in 1895. In the early years of this discovery, the production of X- rays was more focused on the treatment of skin lesions because of the beams physical and biological parameters [4, 5]. In this

present era clinical radiation treatment is known to use linear accelerators or a cyclotron to generate the external beam photon [6]. Medical linear accelerator (LINAC) uses monoenergetic electron beams ranging from 4 to 25 MeV, which produces an X-ray output with a spectrum to energies up to and containing electron energy if electrons are focused on a high density target such as tungsten. External beam photon normally uses Cobalt-60 in the production of photons with an average energy of 1.25MeV for the treatment of cancers. Teletherapy is used in the treatment of various types of tumors including cancers of the head and neck, breast, lung, colon and prostate. The treatment is known to be administered in various fractions from two fractions per treatment to more than fifty fractions for specific prescribed dose [7,8].

From 1987, the International Atomic Energy Agency (IAEA) put out various reports relating to standards in dosimetry and radiotherapy. In two international codes of practice of the absorbed dose to water with Cobalt-60 beam (IAEA TRS 277 of 1987 [9] and IAEA TRS 277 of 1997 [10]), timer error is omitted regardless of its relevance in radiotherapy. Recently, the international codes of practice for the determination of absorbed dose in a cobalt-60 beam, TRS 398 [11] has included the usefulness of timer error evaluation which is established in a worksheet. This worksheet in TRS 398 provides an equation from which dosimetry reading corrected for timer error would be determined. Out of the four well documented timer methods, namely two-exposure method, single/double exposure method, single/multiple exposure method and graphical method [12-19], TRS 398's Code of Practice [11] uses the third method to derive the correction. Recent reviews show that more timer error evaluation will be published as time goes on.

In this experimental work, a Theratron Equinox 100 Cobalt 60 machine is considered for the teletherapy timer error evaluation at the National Centre of Radiotherapy and Nuclear Medicine, Korle Bu. Treatment time calculations (monitor unit) for all teletherapy treatments have been known to factor the timer error as a factor, which accounts for the dose given as the source to travel from the beam off position to the position required for start of treatment. It was hypothesized (Orton et al) that the reliance of output measurements always depended on how well a technique to find a precise approximation of timer error, supposing that every dosimetric instruments are ever so often tested [30]. This work was done to estimate the discrepancy of timer error with the use of graphical method for a Cobalt-60 beam. The timer error value is normally obtained experimentally for an ideal field size of $10 \times 10 \text{ cm}^2$ field size and a depth of 5 cm which is termed as an ideal standard for all treatment cases in dosimetry.

1.2 STATEMENT OF THE PROBLEM

In the manufacture of teletherapy machines, many treatment parameters are entered as raw machine data been programmed collectively for efficient delivery of clinical treatment. During radiation treatment, there are various field sizes that are set for different orientations due to different sites or sizes of tumor within or outside the patient. These differences in diagnosis of sites causes the field size used in the treatment planning procedure (either symmetric or asymmetric) to differ with respect to the patient size. The teletherapy timer error has been known to be one of the retained errors in external beam teletherapy machines. Because teletherapy is known to be treated mostly in fractions an

accumulated error in the shutter error dose calculation can actually go a long way to harm a patient stochastically. In teletherapy, not many studies have been conducted to observe the effects of field sizes and treatment depth on the transit time. Manufacturers across the world have also ignored the treatment time error's dependence on these treatment parameters due to numerous field sizes that can be prescribed out of regular and irregular treatment fields.

There is therefore the need to investigate the dependence of teletherapy timer error in external beam radiotherapy on certain relevant treatment parameters (such as the field size and depth) with the source-surface distance (SSD) technique which is what this study focuses on.

1.3 OBJECTIVES

In view of the importance of the increase in accuracy of dosimetry process for improvement of treatment efficiency; studies were carried out to collect important information for defining a practical standard protocol which would produce precise output estimates for Cobalt-60 teletherapy machines at Korle Bu Teaching Hospital. The primary objective of this research is to evaluate the effect of varying field sizes and treatment depths on timer errors of Cobalt 60 teletherapy unit.

The specific objectives of this research are:

- To determine treatment time errors for different field sizes ($10 \times 10 \text{ cm}^2$, $15 \times 15 \text{ cm}^2$, $20 \times 20 \text{ cm}^2$, $30 \times 30 \text{ cm}^2$) at reference depth of 5 cm.

- To determine the teletherapy timer error at different treatment depths (10 cm, 15 cm, 20 cm, 25 cm, 30 cm, 35 cm and 40 cm)
- To make appropriate recommendations to users of teletherapy equipment.

1.4 RELEVANCE AND JUSTIFICATION

The main purpose of radiotherapy is to deliver a specific amount of dose to tumor and to spare normal tissues surrounding the tumor. Any extra dose given during treatment is considered as not justified. The movement (transit) of source from beam off position to beam on position may vary with respect to treatment parameters and to doses prescribed by physician. In treatment calculations for delivery of dose, all dose prescriptions are converted to timer value with a single field size $10 \times 10\text{cm}^2$ which is the ideal situation. The variation of teletherapy timer error during calculation will allow all irregular field sizes to be converted to a square field size which will correspond to a particular shutter error for a more accurate and precise calculation in treatment timer value for efficient delivery of clinical dose.

1.5 SCOPE OF STUDY

This work is meant to embark on treatment output factors to develop and implement dosimetric protocols for the enhancement of patient treatment and protection at the National Centre of Radiotherapy and Nuclear Medicine (NCRNM) at the Korle-Bu

Teaching Hospital. This is being done by showing the influence of output factors and treatment parameters calculation at various treatment field sizes and treatment depth using a Cobalt 60 Theratron Equinox 100 teletherapy machine. This work's data will be collected by the use of Theratron Equinox 100 teletherapy machine and a large water phantom (tissue equivalent material) manufactured for the teletherapy measurements concerning output factors and treatment parameters. This will be done within a period of two weekends (Saturday and Sunday). Measurements will be taken for separate field sizes of 5×5 , 10×10 , 15×15 , 20×20 , 30×30 and $35 \times 35 \text{cm}^2$ for a constant depth of 5cm and for separate depth of 5, 7, 10, 15 and 20cm for a constant field size of $10 \times 10 \text{cm}^2$.

1.6 ARRANGEMENT OF THE THESIS

The rest of this dissertation is organized as follows; chapter two deals with review of related literature, method and theory are dealt with in chapter three followed by chapter four which presents results and discussion. Finally, chapter five gives summary of the study, conclusions and recommendations.



CHAPTER TWO

2.1 INTRODUCTION

This chapter reviews literature on the treatment timer error relevance on Cobalt 60 teletherapy machines and teletherapy systems as well as some models which are concerned about timer error which is mostly used in clinical teletherapy treatment planning systems and consoles and their effects on the cumulative doses delivered from timer error with its effects on dose prescribed, field size and depth reported by various researchers. The effects of radiation doses caused out of treatment time error on homogenous medium such as water is considered with less relevance to heterogeneities such as the Perspex slabs used in building the water phantom.

2.2 THE COBALT-60 MACHINE

2.2.1 Background

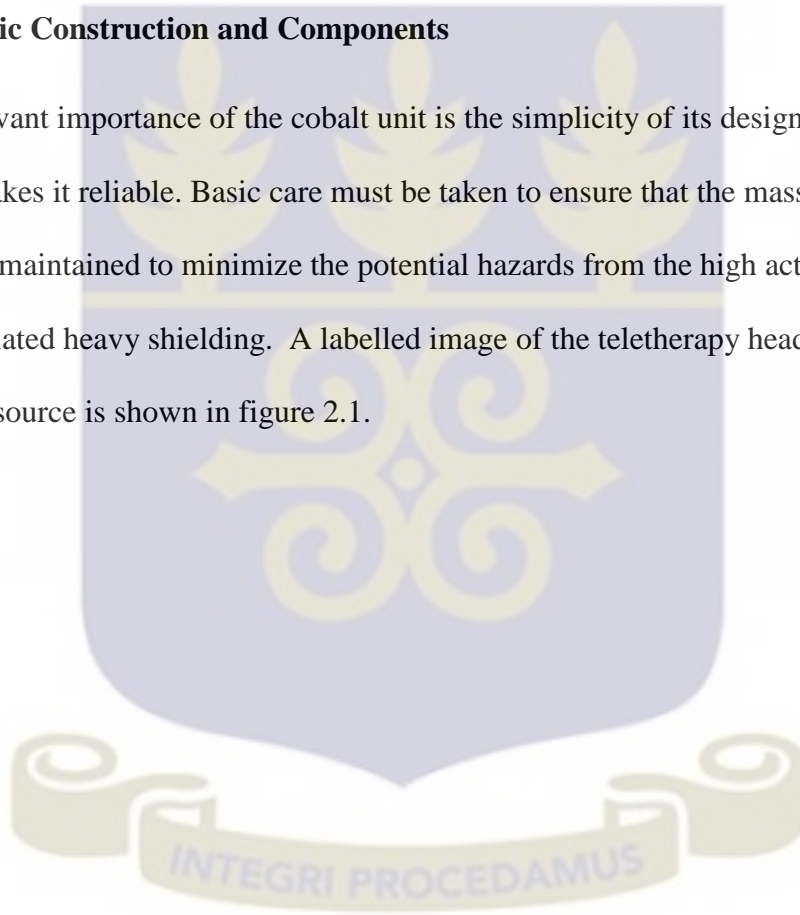
Teletherapy has been known to evolve from Radium therapy to Cobalt-60 teletherapy machines. The findings that an artificial radioisotope might replace radium in the 1970s was a big step in the development of teletherapy [31]. Although megavoltage x-ray units had been available for some years prior to this date, they were not in widespread use, whereas, cobalt units became the mainstay of external beam therapy for the next 30 years or so worldwide. Compared to modern linear accelerators, cobalt units offer poorer geometrical precision in treatment because of a larger penumbra and greater mechanical

inaccuracy [31]. Cobalt can no longer provide the basis for contemporary sophisticated radiation therapy. This is because cobalt beams are less penetrating than those from linacs and they also lack the flexibility in the control of the radiation output offered by linacs. However, commercially available cobalt units may be quite adequate for many non-radical treatments, and there are even some applications where cobalt sources have been used in specially designed equipment to give a performance that could be argued to be superior to that obtainable from a conventional linac [31]. Cobalt-60 therapy is the most appropriate choice for radiotherapy in countries where facilities for the maintenance of linear accelerators (LINACs) are lacking [31]. Many of the major techniques and advances in the physics of external beam therapy were developed on cobalt units. These include arc therapy, conformal therapy, transmission dosimetry, the development and measurement of tissue air ratios and the subsequent derivation of scatter air ratios (SARs), and differential SARs and the associated algorithms for treatment planning based on the separation of primary and secondary radiation. More recently, Poffenbarger and Podgorsak [32] have investigated the possibility of using an iso-centric unit for stereotactic radiosurgery, and Warrington and Adams [36] have shown that conformal therapy, and even IMRT, could be adequately delivered with a cobalt-60 unit except for the most deep-seated tumors [36]. Negligence of the effects of teletherapy timer error with respect to treatment parameters might bring a lot of inaccuracy during the treatment process. The most used models in teletherapy involves rigorous calculation and complicated statistics. The calculations done by a Treatment Planning system is known to be built on fundamental laws of physics and mathematics for the ascertain of numerous computation in developing of the doses required for the Medical Physicist to work

efficiently. These include interaction of particles with matter (photoelectric effect, Compton effect and pair production), statistical analysis and computational comparisons. It is duly noted that the inaccurate specification of interactions the photon has with the matter in transit, the larger the statistical accuracy of predicting their distributions.

2.2.2 Basic Construction and Components

One relevant importance of the cobalt unit is the simplicity of its design and construction which makes it reliable. Basic care must be taken to ensure that the mass fully built and carefully maintained to minimize the potential hazards from the high activity source and the associated heavy shielding. A labelled image of the teletherapy head showing the standard source is shown in figure 2.1.



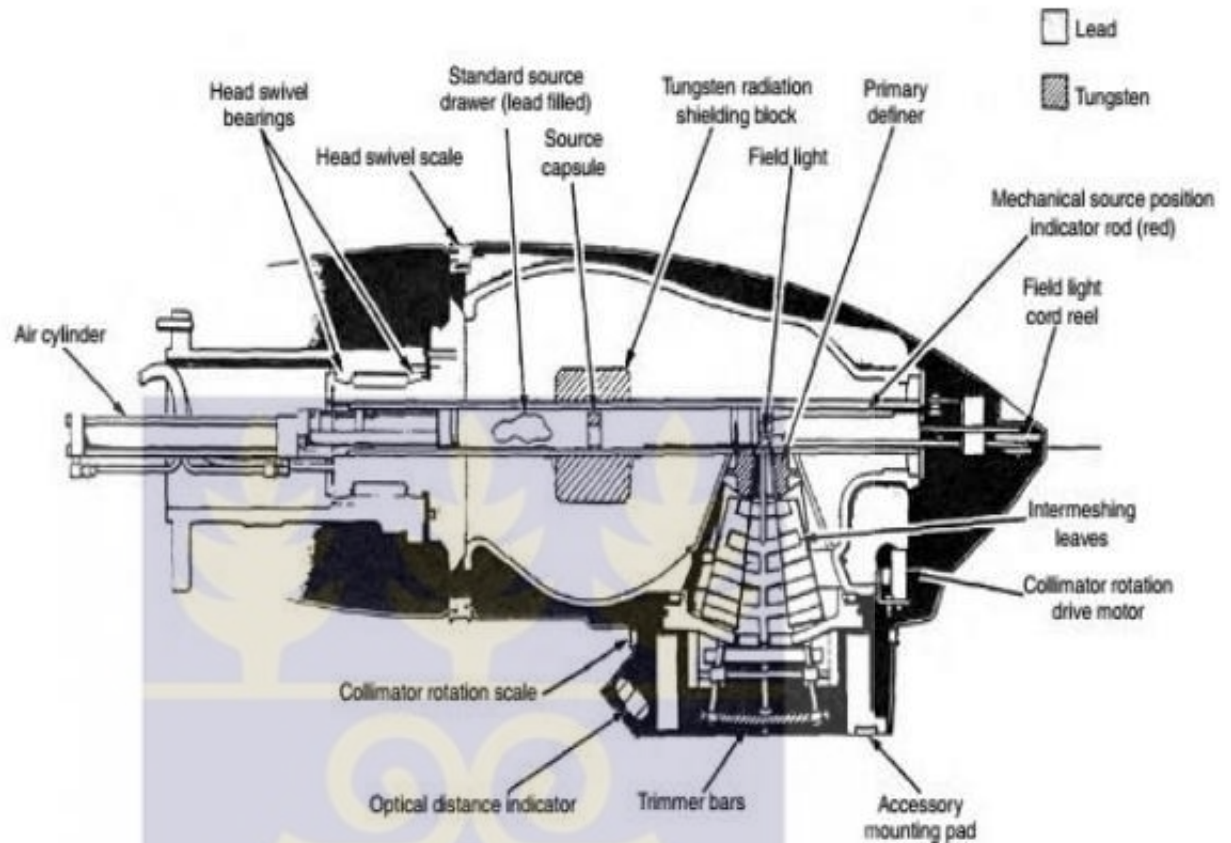


Figure 2.1: A diagram showing inside the head of a teletherapy gantry [20]

2.2.2.1 The Head

Where the teletherapy source is being kept or housed is called the source head. This consists of a steel shell with lead for shielding purposes and a mechanism for transporting the source in front of the collimator outlet to produce the clinical ray beams.

- There are two mechanisms developed in the transport of the source from beam off position to beam on position and reverse;
 - i) a source on a sliding drawer and

ii) a source on a rotating cylinder.

- At beam off position, of the source, a light appears in the beam on position above the collimator opening, enabling an optical visualization of the radiation field which is defined by the collimator system.

- Radiation cannot be stopped completely because of this; some radiation will escape from the unit when the source is at the beam off position. It is known to tolerate a high leakage of 1mR/h at 1m from the source. Intervention regulations require that the average leakage of a teletherapy machines is less than 2mR/h [21].

2.2.2.2 The Source

One of the primary sources used in teletherapy machines are gamma(γ) ray sources.

These are designed and built sources which comprises of a suitable, artificially produced radioactive material. In the production of γ rays, firstly the parent source undergoes a β decay, which results in an excited daughter nucleus which attains ground state through emission of γ rays.

The vital attributed of radioisotopes for EBRT are:

- High γ ray energy;
- High specific activity;
- Relatively long half life
- Large specification air kerma rate constant

The most used teletherapy source uses cobalt 60 radionuclides construct inside a cylindrical stainless steel capsule and sealed by welding. A double welded seal is used to prevent any leakage of the radioactive material. The source is known to be cylindrical which has a diameter ranging from 1 to 2cm; with a height of the cylinder about 2.5cm being a compromise between achieving a high or sufficient activity to obtain a reasonable output and keeping the source small enough to minimize the beam penumbra. The smaller the source diameter, the smaller the physical penumbra and the more expensive the source [21, 22]. The space behind the active cobalt material in the capsule must be tightly packed with blank discs to eliminate movement. The low energy beta ray emission from the source is filtered out by the capsule walls.

2.2.2.3 Gantry

In order to obtain a reasonable compromise between output, depth dose, and clearance around the patient, modern cobalt units are manufactured in a standard iso-centric configuration with a source axis distance of 80cm being the most common [31]. Units with an SAD of 100cm are also practical if high activity sources can be afforded and offer the advantages of greater depth dose, larger field sizes, greater clearance around the patient, and geometrical compatibility with linacs. In order to increase their versatility, iso-centric units have often been made with the ability to swivel the head about a horizontal axis through the source. This swivel motion keeps the beam axis in a vertical plane, and when used with an appropriate gantry angle, may be useful for extended SSD treatments or for treating immobile patients in a bed or chair. Some non iso-centric cobalt

units have been manufactured with the head held by a yoke on a vertical stand, and these are particularly useful for giving single field palliative treatments. Where an iso-centric unit has the swivel facility, great care must be taken to ensure that its position is accurately reset before the equipment is used for normal iso-centric use since the slightest angulation of the head swivel will create a large deviation of the beam axis from the mechanical iso-center. Some iso-centric units use slip rings for the supply of all power and control signals to the gantry and this allows continuous gantry rotation. Coupled with the guaranteed constant output from the source as the unit rotates, such a versatile and simple rotation mechanism provides an ideal unit for arc or full rotation therapy when this technique is required [31]. This is the path of the cobalt 60 machine that holds the source head. It is manufactured in a way that makes it rotatable to a degree of $\pm 180^\circ$. It is affixed on the housing of the base. Most modern gantry systems are known to have an indicator of source position on it to provide the user with insight of what is happening during the treatment or using process. The gantry also possesses the collimator which serves as the definition of the opening of the source [22].

2.2.3 Beam modifiers

Beam modifiers are known to comprise of jaws, wedges, blocks, compensators, multileaf collimator (MLC), electron cutout and bolus. These are devices or materials that are included or factored in dose calculation in radiation treatment planning. Most are used in the simulation process before treatment is delivered either through the treatment planning

system or the simulator. The four main uses of beam modifiers are for shielding, compensation, wedge filtering and beam fattening.

In shielding, the beam modifier is used to eliminate radiation to a part of the field or a zone that the beam is directed to;

For compensation, it is used to achieve a uniform dose for the treated zone.

When the beam enters obliquely through the body or where there is a tilt or curves wedge filtering is needed for treatment.

For flattening, it helps with the spatial distribution of the natural beam. It is altered by reducing the central exposure rate relative to the peripheral. These beam modifiers factor in to doses given through source transit if they are present during the treatment process [23, 24].

2.3 OUTPUT FACTORS

Output factors comprise of the beam data used in the commissioning of the EBRT machine. The values of the output factors are gotten through a series of measurements performed after installation of the equipment. This beam data is inputted in to the treatment planning system (TPS) for beam calculations during treatment planning. The output factors are always obtained by the variation of one or more treatment parameters such as field size and treatment depth during experimental work or beam data collection. The output factor can be determined as the ratio of corrected readings measured under a

given set of non-reference conditions to that measured under reference conditions. Timer error is an output factor determined during the experimental process [25].

2.4 Collimator system

The collimator system is normally the outlet of the beam for which a definite field size can be determined or set through the treatment console. The collimator system is mostly made up of four bars called jaws. These jaws are stacked one on the other to create a rectangular or square shape to prevent interference during movement. The jaws are usually made of a material with high atomic number (z) either tungsten or lead. It is sometimes used in advanced external beam systems to seal out the source completely in case the source gets stuck during treatment. The gamma ray source upon hitting the collimator sometimes produces electrons that interfere with treatment time and timer error doses.

An advancement in the collimator system recently, is the use of multileaf collimator systems. This is a technology improvement which has been manufactured for the replacing of the use of lead blocks or cerrobend Tm blocks attached to the tray during treatment. The collimator system has an opening for some beam modifiers such as wedges and tray to be inserted for comfortable treatment since it is noninvasive to patients [26, 27].

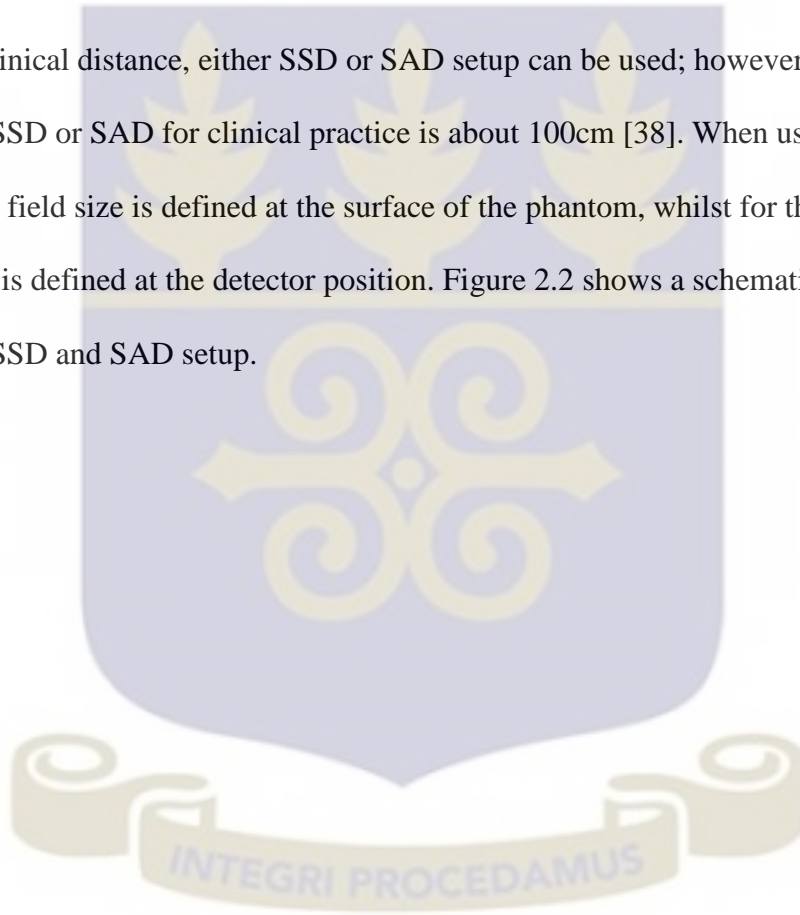
2.5 Treatment Parameters

There consist of a series of parameters that affect precise patient treatment. These may include field size, treatment depth, collimator angle, gantry angle and treatment cache angle. When an electron or photon beam is incident on a patient or phantom, the absorbed dose varies with depth and depends on energy, field size, SSD or SAD, and beam collimation system. The calculation of dose in the patient affects depth dose distribution with regard to these parameters [37]. In this report, discussion of treatment parameters is going to be in the context of treatment planning; however, the central axis depth dose distribution will not be sufficient to characterize a radiation beam that produces a dose distribution in a three-dimensional volume. In view of this, lines passing through points of equal dose (known as isodose curves) are used to represent volumetric variation in absorbed dose and dose distribution [37]. These curves are usually drawn at regular intervals of absorbed dose and are expressed as a percentage of the dose at a reference point. Thus, the isodose curves represent levels of absorbed dose in tissue.

2.6 Source to surface distance (SSD) and Source to axis distance (SAD)

Source size, SSD, and SAD all affect the shape of isodose curves by virtue of the geometric penumbra [37]. SSD also affects the percent depth dose and therefore the depth of the isodose curves. Dose variation across the field border is a complex function of geometric penumbra, lateral scatter, and collimation; thus, the field sharpness at depth is

not simply determined by the source or focal spot size. For example, by using penumbra trimmers or secondary blocking, the isodose sharpness at depth for cobalt-60 beams with a source size less than 2cm in diameter can be made comparable with higher-energy linac beams, although the focal spot size of these beams is usually less than 2 mm. Comparison of isodose curves for cobalt-60, 4MV, and 10MV illustrates the point that the physical penumbra width for these beams is more or less similar. It has to be noted that at any normal clinical distance, either SSD or SAD setup can be used; however, the mostly used value of SSD or SAD for clinical practice is about 100cm [38]. When using the SSD setup, the field size is defined at the surface of the phantom, whilst for the SAD setup, the field size is defined at the detector position. Figure 2.2 shows a schematic diagram of both the SSD and SAD setup.



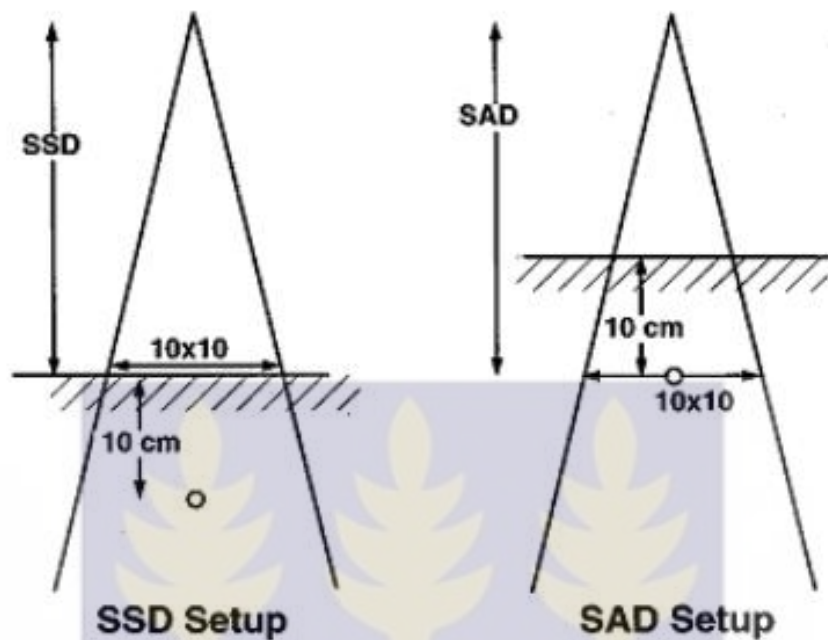


Figure 2.2: Schematic diagram of the SSD or SAD setups which may be used for photon beam reference dosimetry for equivalent depth.

2.7 Field Size

Field size is one of the most important parameters in treatment planning. Adequate dosimetric coverage of the tumor requires a determination of appropriate field size. This determination must always be made dosimetrically rather than geometrically. In other words, a certain isodose curve (e.g. 93-95%) enclosing the treatment volume should be the guide in choosing a field size rather than the geometric dimensions of the field [34, 37]. Great caution should also be exercised in using field sizes smaller than 6cm in which a relatively large part of the field is in the penumbra region. Depending on the source

size, collimation, and design of the flattening filter, the isodose curves for small field sizes, in general, tend to be bell shaped. Thus, treatment planning with isodose curves should be mandatory for small field sizes. The isodose curvature for Cobalt-60 increases as the field size becomes overly large unless the beam is flattened by a flattening filter [37]. The reason for this effect is the progressive reduction of scattered radiation with increasing distance from the central axis as well as the obliquity of the primary rays. The effect becomes particularly severe with elongated fields such as cranial spinal fields used in the treatment of medulloblastoma. In these cases, one needs to calculate doses at several off-axis points or use a beam-flattening compensator [34].

2.8 EFFECTS AND REVIEW OF TIMER ERROR

From vigorous researching, it was noted that no work had been done on the determination of timer error in variation to field size and treatment depth for Cobalt 60 machines. These are works that talk mostly about the determination on timer not purposely with dependence on field size and treatment depth.

Firstly, considering a report released by IAEA in 2001 on misadministration in external beam radiation. The report indicated that one of the pre- dominant causes of misadministration in radiation therapy is calculating error of exposure time in dose delivery. After the doctor has prescribed dose to be administered to patient and the radiotherapist has determined field size and depth, medical physicists then calculate the

time of exposure. Different cancer type and stage have different field size and depth prescriptions which affect the time of exposure and in turn affect the timer error so it is therefore not advisable to add the use on definite timer error for all clinical treatments [28].

Besides the report released by IAEA, ICRU in its report No. 24 also suggested that an uncertainty of 5% is required in the delivery of absorbed dose to the target volume because of shutter time error. Timer error has been identified as one of the parameters that must be determined. It is necessary to consider timer error in dose delivery to get correct dosimeter reading rate or absorbed dose to patient.

Samat et al on (2008) “the determination of timer error and its role in the administration of specified dose” used the graphical method in the determination of timer with variation to doses. This method used or adapted in my experimental research work. She found that a general timer error of 1.28s should be added to every patient’s calculated clinical treatment time to reduce dose uncertainty which stays as a constant value for a period of treatment. Because of no adaptation of her results to treatment parameters such as field size and depth, it was only her method that was used during the data analysis of this experimental work [29].

The comparison of two standard dosimetry protocols for output calibration for Cobalt 60 teletherapy machines also published by C. Tannanonta et al in Thailand in” The measurement of teletherapy unit timer errors” elaborates on the importance of the determination of teletherapy timer error in air and in water using both short exposure time and long exposure time. Their timer error was determined by two methods proposed by Orton and Seibert [30]. The methods as shown in equation 2.1 and 2.2.

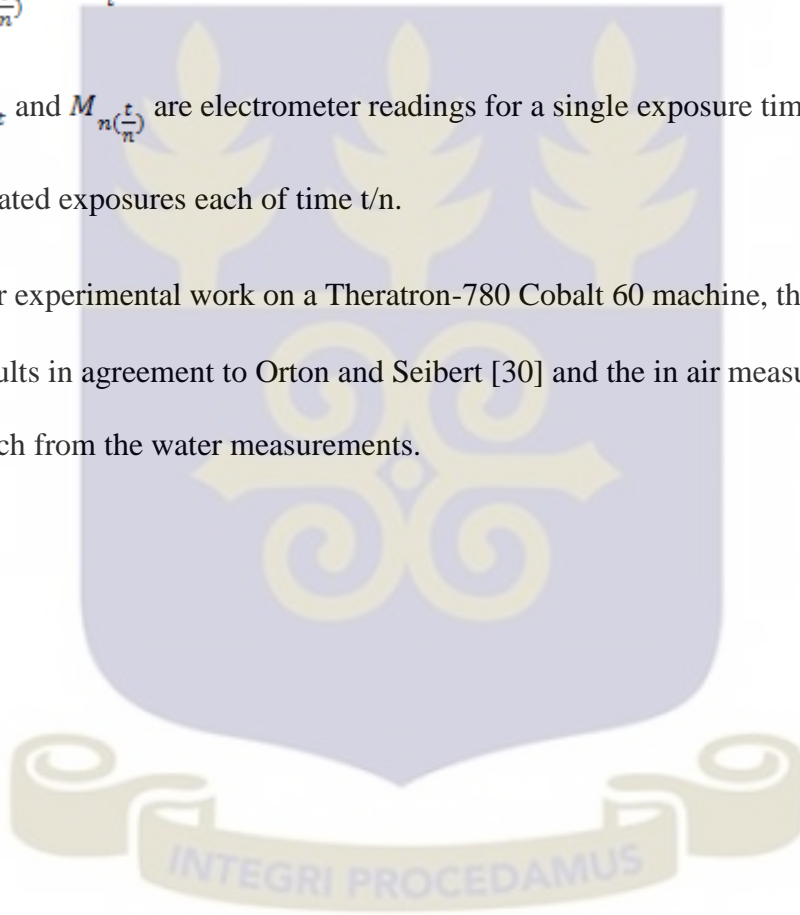
$$e = \frac{t_s M_l - t_l M_s}{M_s - M_l} \dots \dots \dots (2.1)$$

Where t and M are exposure time and meter reading and subscript s and L are the short and long exposure time.

$$e = \frac{t(M_l - M_{n(\frac{t}{n})})}{M_{n(\frac{t}{n})} - nM_t} \dots \dots \dots (2.1)$$

Where M_t and $M_{n(\frac{t}{n})}$ are electrometer readings for a single exposure time t and n which are integrated exposures each of time t/n.

With their experimental work on a Theratron-780 Cobalt 60 machine, the t_s and t_l had better results in agreement to Orton and Seibert [30] and the in air measurements did not differ much from the water measurements.



CHAPTER THREE

MATERIALS AND METHODS

3.1 MATERIALS

Equipment used for this study include the Theratron Equinox 100 Cobalt 60 unit, full water scatter phantom, Farmer type ion chamber and electrometer, thermometer and barometer.

In the measurement of the teletherapy timer error during treatment, different field sizes and treatment depths were used. The experiment was performed using a full water scatter phantom which simulated a human (patient). The ion chamber connected to an electrometer (serial number T10008-08112, PTW, Freiburg, Germany) was used for the radiation measurements when the water phantom was irradiated. The radiation measurements were corrected for environmental conditions of temperature and pressure. Figure 3.1 (a) and Figure 3.1 (b) are the digital thermometer and barometer used in the study respectively.



Fig 3.1(a): Digital thermometer



Fig 3.1(b): Barometer

3.1.1 Theratron Equinox 100 Co-60 teletherapy unit

The Theratron Equinox 100 Co-60 teletherapy unit, as shown in Figure 3.2, is used for radiation therapy at the NCRNM, KBTH. This unit was manufactured by Theratron and acquired from Canada with a model number 2117. The Equinox teletherapy unit is led by a rotatable gantry and collimator. It works together with a unit head panel, hand control and control console with display monitor as shown in Figure 3.3. The radioactive source, Cobalt-60 is moved from a shield safe located inside the gantry (safe position which is a double layer stainless steel capsule such that the diameter of the whole source assembly is 2.0 cm and 3.0 cm long) and brought in the collimator position in the treatment process. The teletherapy unit is a modern computerized system with a Prowess Panther treatment planning software which runs on a Microsoft Windows computer and is configured according to the specific regional setting. This software uses Computed tomography image slices to calculate doses according to physician contour drawings which in turn is used for medical physicists planning discretion.



Fig 3.2: The Theratron Equinox 100 Cobalt 60 machine at Korle Bu

3.1.2 Farmer type ionization chamber

A waterproof Farmer type ionization chamber which is 0.6 cm^3 in volume was used in this study. The chamber is made by PTW Feiburg, Germany with model number TM 30013 and serial number 005801. The ionization chamber used was calibrated against a source of known beam quality at the IAEA Secondary Standard Dosimetry Laboratory (SSDL). The calibration was done with a bias voltage of 400 V at the temperature of 293 K 20°C , pressure of 101.325 kPa and humidity of 50%. Figure 3.4 shows the 0.06 cc ionization chamber.



Figure 3.4: The PTW UNIDOS electrometer

3.1.4 2-Dimensional Water phantom

An in-house manufactured manual two-dimensional (2-D) water phantom was used during this research. The phantom was manufactured from poly-methyl methacrylate (PMMA) material, with reference dimensions of 70 cm × 70 cm × 45 cm for teletherapy experimental work (AAPM TG 106 [33]). The phantom is constructed in such a way that scatter is minimized to a greater degree. The phantom has a holder which is designed to hold ionization chamber laterally in the water. This holder is also designed with a

cylindrical PMMA with mechanical gears for easy movement and it possesses rigid holding capabilities. The phantom has a height graduation reader which helps in the depth readings. The phantom was used to measure the transit time dose to water at different depths and different field sizes.



Figure 3.5: Large water phantom

3.1.5 SOFTWARE

The Microsoft excel software produced by Microsoft Corporation was used for the compiling of the data into tables and the drawing of the graphs used in this work. It is a high performance spreadsheet analyzer for technical analysis. It enabled the determination of gradients and various intercepts of the graphs and created mathematical solutions for various equations used in the completion of this project.

3.2 METHOD

3.2.1 Stability check

The stability of the farmer type ionization chamber was confirmed with a long-life radioactive source for long time stability. The stability check source is used to check the constancy of the ionization chamber and to verify that no significant change has occurred since the calibration from laboratory. The long-life check source used in this case was Sr-90 / Y-90 encapsulated in silver foil. This is known to be a pure beta-particle emitter (emits electrons only). The half-life of the Sr-90 is 28 years and the Y-90 beta particle has an energy of 2.2 MeV which is adequate to penetrate the silver foil and the chamber foil.

The ionization chamber was then placed in the chamber. All readings were corrected for atmospheric conditions at the chamber position.

Set limit for the relative standard deviation of the check source reading, determined from repeated measurements, was 0.5 % from baseline values established for the source/chamber/electrometer assembly [11].

3.2.2 General Procedure and Experimental Setup

The water phantom was first placed on a bed with a stable support with a lifter which when adjusted brought the phantom to a height close to a treatment set up. It was then filled with about 250 liters of water which filled it to a reference mark on the phantom. The digital thermometer was clung to one side of the phantom with the metallic sensitive

part in the water. The barometer was also placed on a table in the treatment room. The water was then left for a few hours for the adjustment of stability of temperature and pressure conditions as shown in Fig 3.7. After a stable environmental condition was established, both the horizontal and vertical lasers were checked for correspondence with the phantom reference laser markings as shown in Fig 3.6.



Fig 3.6: Laser setup during experimental work

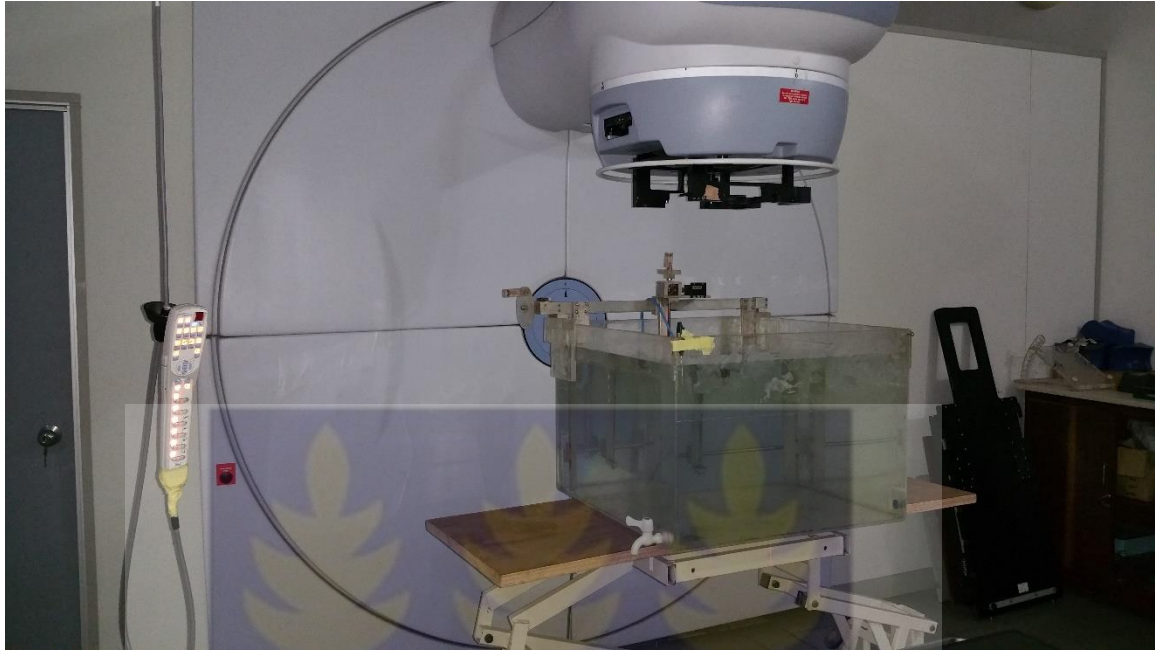


Fig 3.7: General experimental Setup



Fig 3.8: Treatment Control Console



Fig 3.9: Chamber holder used during this experiment

The ion chamber was fixed in the chamber holder (Figure 3.9) of the water phantom making sure there was no movement possible when readings are taken. The sensitive section of the ionization chamber was lowered into the water phantom ensuring that the tip was at an SSD of 100 cm, which is the defined SSD of the machine at the surface of the skin. The electrometer was then connected to the ionization chamber with its special cable. A treatment time of five minutes as shown in fig 3.8 was then set to irradiate and warm up the ionization chamber for preparation of readings at a depth of 0.5 cm which is known as the point at which maximum dose is given and a large field size of $30 \times 30 \text{ cm}^2$.

3.2.2.1 Measurements with varying field sizes

The ionization chamber was then lowered into the water to a treatment depth of 5 cm from the surface of the water in the phantom. A field size of $5 \times 5 \text{ cm}^2$ was set on the treatment console together with other beam parameters as shown in Fig 3.8. After beam parameters were set using the console the machine's remote control or navigator in the treatment room was used to move and confirm these parameters. The gantry angles and collimator angles were kept at a constant 0° . The electrometer was then set to start (STA button) before every reading taken in order to measure doses when the source was in transit. The treatment timer on the console (Fig 3.7) was set to treatment times of 0.5 min, 1.0 min, 1.5 min, 2.0 min, 2.5 min and 3.0 min for this setup. Two electrometer readings were taken for each timer setting. The thermometer readings were recorded before and after every batch (treatment timer changes) of measurements. The barometer reading was taken at the beginning and end of the whole experimental work. The set-up was repeated with a variation in the field size for field sizes of $10 \times 10 \text{ cm}^2$, $15 \times 15 \text{ cm}^2$, $20 \times 20 \text{ cm}^2$, $30 \times 30 \text{ cm}^2$, $35 \times 35 \text{ cm}^2$. The sleeves of the collimator could be set to a maximum field size above $35 \times 35 \text{ cm}^2$ but no patient has ever been treated with such a large field size in Ghana so far which was advised to be ignored. All the readings were recorded for analysis.

3.2.2.1 Measurements with variations of varying treatment depths

For the measurement of the variation of depth, the field size was set at a constant $10 \times 10 \text{ cm}^2$. The ionization chamber was then lowered into the water with the mechanical gear attached to the chamber which counts 70 turns equivalent to 1 cm. 350 turns was set which corresponded to a treatment depth of 5cm from the surface of the water in the phantom. A field size of $10 \times 10 \text{ cm}^2$ was set on the treatment console together with other beam parameters. After the beam parameters were set-up using the console, the machine's remote control or navigator in the treatment room was used to move and confirm these parameters. The gantry angles and collimator angles were kept at a constant 0° . The electrometer was then set to start (STA button) before every reading was taken in order to take into account doses when the source was in transit. Two electrometer readings were taken for each timer setting. The treatment timer on the console was set to treatment times of 0.5 min, 1.0 min, 1.5 min, 2.0 min, 2.5 min and 3.0 min. The thermometer readings were recorded before and after every batch (treatment timer changes) of measurements. The barometer reading was taken at the beginning and end of the experimental work. This set-up was repeated with a variation for the vertical mechanical counter for counts of 490 equivalent to 7 cm depth, 700 equivalent to 10 cm depth, 1050 equivalent to 15 cm depth and 1400 equivalent to 20 cm depth. All the readings were recorded on paper during every change of depth in the process.

3.3 DATA ANALYSIS

Because of the bulky data acquired, Microsoft excel was used to process the data from the measurements made. Microsoft excel professional plus 2016 was the version used to compute the mean electrometer readings, temperature and pressure during this experimental work. Microsoft excel was used to calculate for the corrected readings, the gradient and intercept. The program was also used to plot and analyze required graphs for this work.

3.3.1 CALCULATIONS AND GRAPH PLOTTING

After all readings were taken the mean value of the two readings was obtained from the formula as shown in equation 3.1 below.

$$\text{Mean(Average)} = \frac{x_1 + x_2}{n} \dots\dots\dots(3.1)$$

Where x_1 = first electrometer reading

x_2 = second electrometer reading

n = number of data

The average readings were then corrected for environmental conditions of temperature and pressure with the use of a formula obtained in the TRS 398 [28] as shown below.

$$k_{TP} = \frac{(273.2 + T) P_0}{(273.2 + T_0) P} \dots\dots\dots(3.2)$$

Where k_{TP} = correction factor

T_0 = initial temperature

T = final temperature

P_0 = initial pressure

P = final pressure

$$\text{Mean corrected reading} = \text{mean reading} \times k_{TP} \dots \dots \dots (3.3)$$

The mean corrected readings were then plotted on the y-axis against the timer variations on the x-axis for the various variations in field sizes and depths. The graph generated was straight line plot which has the general equation;

$$y = mx + c \dots \dots \dots (3.4)$$

Where y = y-axis value

m = gradient

x = x-axis value

c = intercept

$$m = \frac{y_2 - y_1}{x_2 - x_1} \dots \dots \dots (3.5)$$

The equation of a straight line was calculated for each graph using excel formulas as shown in equations 3.5. Both the y-intercept and the slope can also be gotten from the graph. The teletherapy timer error is equivalent to the x-intercept for each variation which can be gotten after the equation of straight line is evaluated. It is the x-axis value for which y = 0. Therefore, the formula for attaining it is shown in equation 3.6 and 3.7.

$$0 = mx + c \dots\dots\dots (3.6)$$

Making x the subject

$$x = \frac{-c}{m} \dots\dots\dots (3.7)$$



CHAPTER FOUR

RESULTS AND DISCUSSION

4.1 INTRODUCTION

This chapter discusses the results obtained from the measurements in the study. Six field size variations and five depth variations were used throughout the experimental process. All measurements were taken as in water.

4.2 DEPENDENCE ON FIELD SIZE

From the measurements taken, the data for the computation of the mean measurements of two readings corrected for temperature and pressure with respect to the timer value of the console can be seen in Appendix A for a treatment depth of 5 cm. The graphs for the plotted corrected readings against time can also be found in Appendix C. The equation of a straight line for each variation was developed with the help of an Excel algorithm which can also be seen in the graphs of Figure 4.1, 4.2 and Appendix C. The graph produced a straight line because the corrected electrometer reading (Dose) is directly proportional to the treatment timer value hence the more time the beam is on the more the radiation received by the ionization chamber or patient. Although Excel produced the equation of the straight line from the data obtained, to determine the timer error, a manual equation was fed into it to compute the x-intercept. The x-intercept was calculated with an equation of the ratio of the y-intercept and the gradient (which was found to be a

negative value for each variation in field size). From the timer errors obtained as shown in Table 4.1, the values varied to a degree of 10^{-2} which is significant in radiotherapy, because small amount of timer error can go a long way to harm a patient during treatment. All the error values estimated were negative which means that the timer errors should be subtracted from the timer value estimated from the prescription before clinical treatment is carried out.

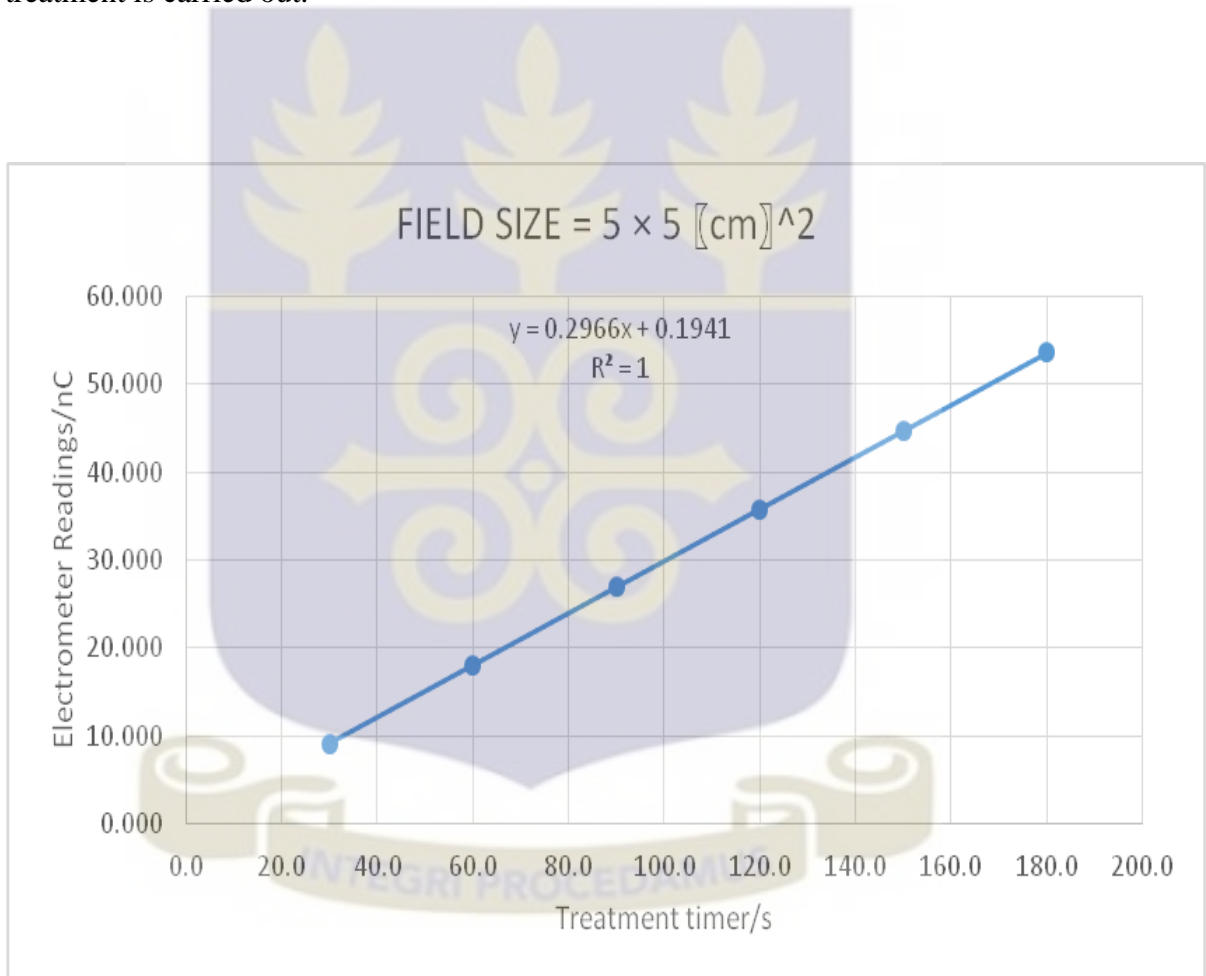


Figure 4.1: A graph of corrected electrometer reading against treatment time for a 5×5 cm² field size

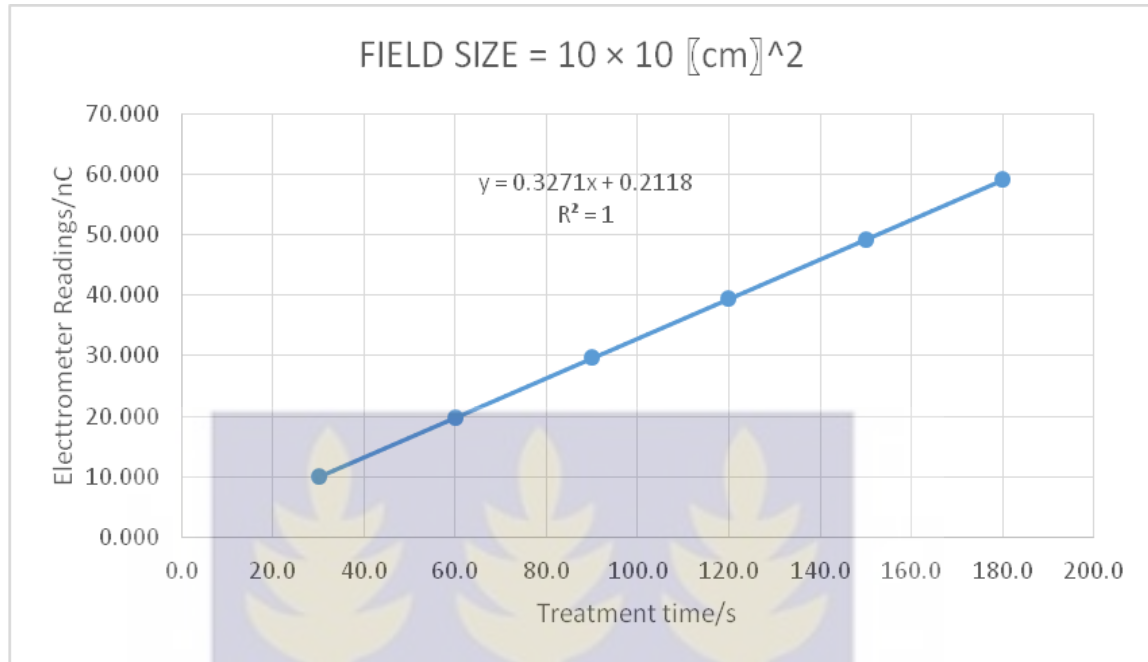


Figure 4.2: A graph of corrected electrometer reading against treatment time for a $10 \times 10 \text{ cm}^2$ field size

Table 4.1: Field size with timer errors obtained for their setup

Square Field Size / [cm] ^2	Timer error (s)
5×5	-0.654
10×10	-0.648
15×15	-0.622
20×20	-0.633
30×30	-0.639
35×35	-0.643

Figure 4.3 shows the variations of timer error with field size, giving a polynomial function of the fifth order which was; $y = 2E-07x^5 - 2E-05x^4 + 0.0008x^3 - 0.0137x^2 + 0.0976x + 0.4198$. This shows the degree of irregularity in the dependence of teletherapy timer error on field size. The source's beam is made up of a primary and scattered component. The primary beam is known not to vary with field size but the scattered beam varies with field size [34]. It was observed that as the field size increased from 5×5 to 15×15 the teletherapy timer error decreased from a value of 0.65s to 0.62s. The sources of scatter include the collimator, blocks and wedges in the beams path. At lower field sizes the beam hits the collimators before a path is created during treatment so the intensity of collimator scatter is increased. As the field size is increased from 15×15 to 35×35 there is an increase in the timer error. This increase is produced as a result of increasing phantom scatter. The scattered beam is a product of the collimator scatter and phantom scatter as shown in equation 4.1 [35].

$$S_{cp} = S_c \times S_p \dots\dots\dots 4.1$$

Where S_{cp} = total scatter correction factor

S_c = collimator scatter correction factor

S_p = phantom scatter correction factor

As the field size increased above 15×15 the effect of the phantom scatter factor outweighs the collimator scatter factor. This phantom scatter factor increases with increasing field size. The values calculated for timer error can be varied during every treatment calculation by the conversion of irregular field sizes to equivalent square field

sizes. Corresponding timer errors of the equivalent field sizes are subtracted during the calculations. This enhances treatment output factor's efficiency during treatment.

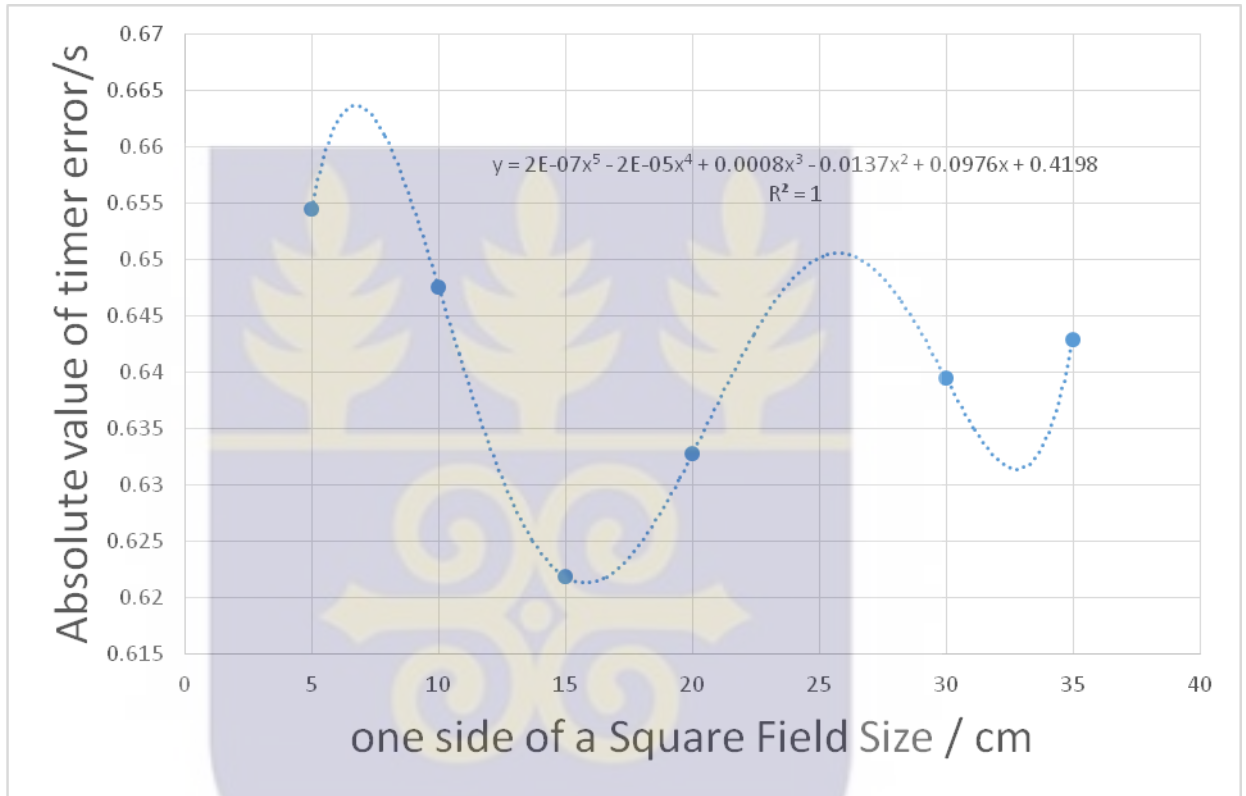


Figure 4.3: A graph showing the dependence of timer error on field size

4.3 DEPENDENCE ON TREATMENT DEPTH

Data for the computation of the mean of the two readings corrected for temperature and pressure with respect to the timer value of the console can be seen in Appendix B for a constant field size of $10 \times 10 \text{ cm}^2$. Their corresponding graphs for were plotted for corrected electrometer readings in nC on the y-axis against time in seconds on the x-axis which can also be found in Appendix D. An equation of a straight line for each treatment depth variation was developed with the help of a Microsoft Excel algorithm which can also be seen in graphs at Fig 4.4, 4.5 and Appendix D. The graph produced a straight line because the corrected electrometer reading (Dose) is in direct relation to the treatment timer value hence the more time the beam is on the more the radiation received by the ionization chamber or patient. The x-intercept was obtained by putting $y = 0$ for an input equation put into Microsoft Excel. The teletherapy timer error was calculated with an equation of the ratio of the y-intercept and the gradient (which was found to be a negative value for each variation in depth too). From the timer errors obtained as shown in Table 4.2, the timer error values varied to a degree of 10^{-1} which is more noteworthy in radiotherapy and can affect the perceived effects of treatment prescription since there is an unknown additional dose during delivery. All the teletherapy timer (shutter) error values obtained was a negative which means that the timer errors should be subtracted from the timer value calculated from the prescription before clinical treatment is carried out.

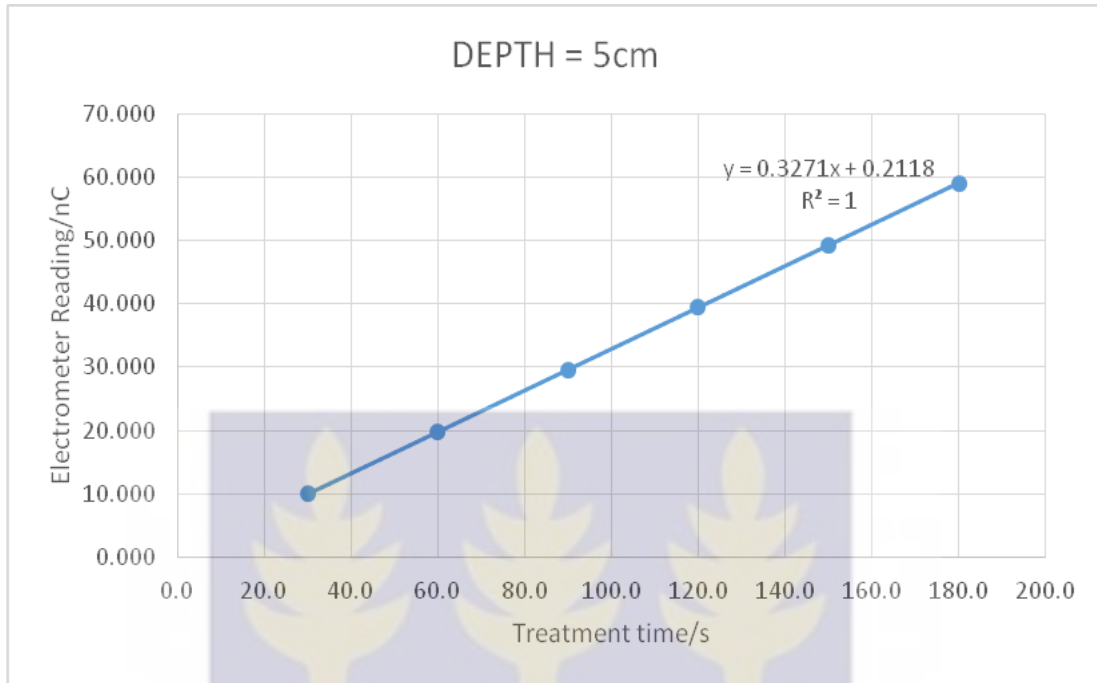


Figure 4.4: A graph of corrected electrometer reading against treatment time for a 5cm depth

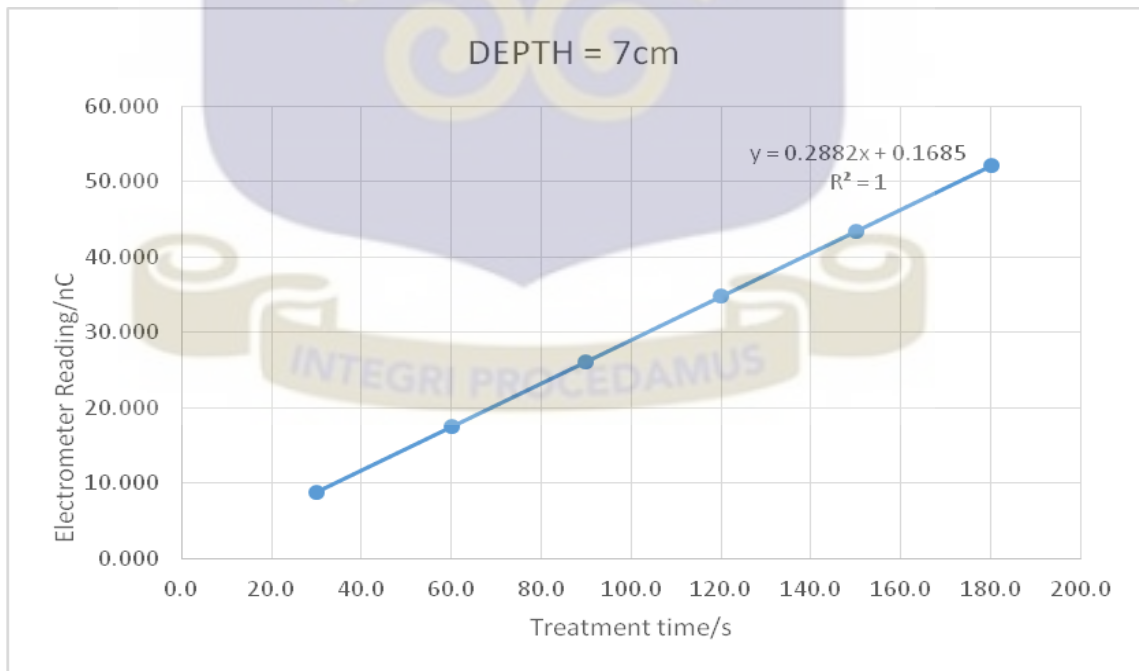


Figure 4.5: A graph of corrected electrometer reading against treatment time for a 7cm depth

Table 4.2: Treatment depth with timer errors obtained for their setup

Treatment depth (cm)	Timer error (s)
5	-0.648
7	-0.584
10	-0.612
15	-0.665
20	-0.621

The absolute values of the timer error were plotted against the variation in treatment depth as shown in Figure 4.6. Figure 4.6 shows the variations of timer error with depth giving a polynomial function of the fourth order as $y = 4E-05x^4 - 0.0023x^3 + 0.0456x^2 - 0.362x + 1.5825$. This elaborates the degree of irregularity in the dependence of teletherapy timer error for varying treatment depth. It was witnessed that as the treatment depth changed from 5 cm to 7 cm there was a decrease in the absolute value of timer error. This is as a result of electron contamination. Electron contamination normally occurs as a result of electrons produced from the interaction of the Cobalt-60 photons with a high z material (usually the collimator) and air (through ionization and production of secondary electrons). The ionization chamber at shallow depths measure both photons and electrons because electrons are not attenuated at shallow depths. After this decrease the teletherapy timer error increased from a depth of 7 cm through depths of 10 cm to 15 cm which was the highest value of timer error obtained as 0.67 seconds. The increase in

timer error is as a result of scattering as the ionization chamber detects radiation deeper in the water medium as shown in Figure 4.6. The teletherapy timer error decreased again from a value of 0.67s to 0.62s. At higher depths there is beam attenuation which can account for the decrease in timer value. Also the lack of back scatter can cause this since the ionization chamber requires an amount of material to be present beneath it before back scatter can occur. The values calculated for timer error can be varied during every treatment calculation by the variation in the value for each treatment depth corresponding to teletherapy timer error subtracted during timer value calculation which will also enhance treatment output factor's efficiency during treatment.

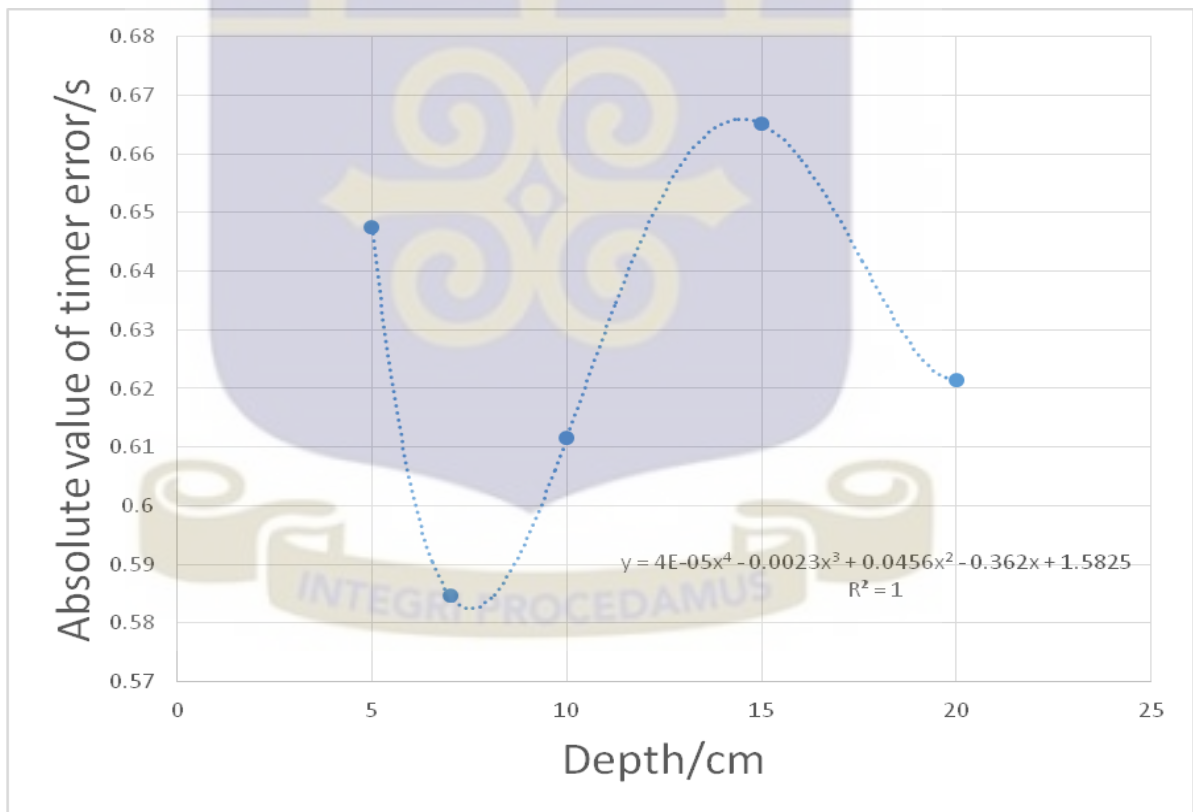


Figure 4.6: A graph showing the dependence of timer error on treatment depth

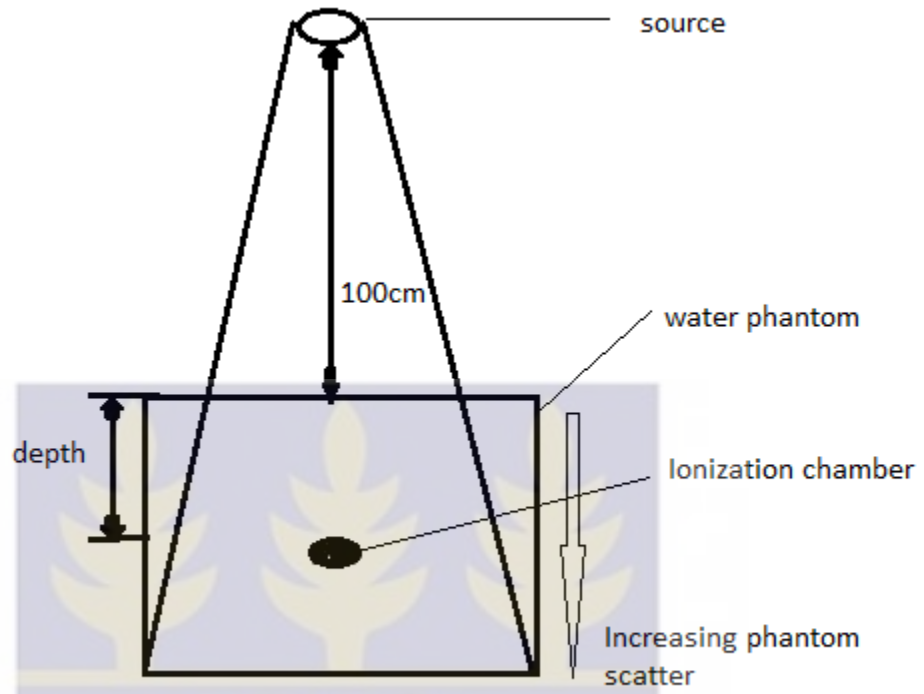
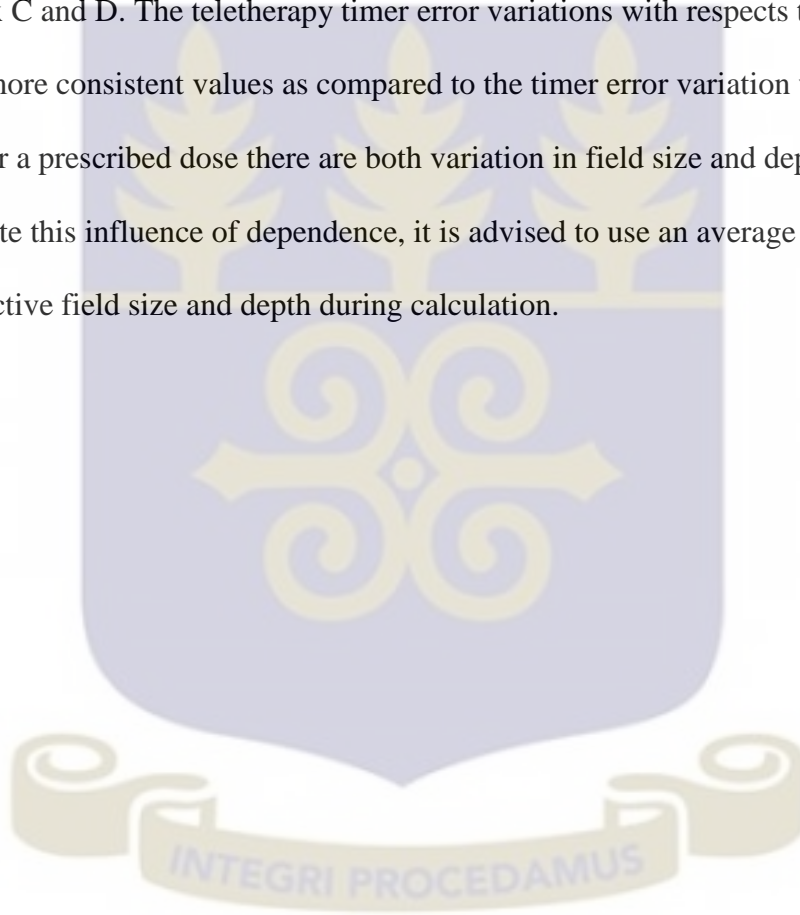


Figure 4.7: Diagram showing increasing phantom scatter.



4.4 COMPARISON BETWEEN FIELD SIZE AND DEPTH

In this work the teletherapy timer error determined for both treatment parameters considered (field size and depth), had little variations in the order of 10^{-2} and 10^{-1} . Due to the linearity of the ionization chamber, the individual variations allowed a straight line to be used for determination of the correspondence with Samat et al [29] as shown at Appendix C and D. The teletherapy timer error variations with respects to field size showed more consistent values as compared to the timer error variation with treatment depth. For a prescribed dose there are both variation in field size and depth so in order to incorporate this influence of dependence, it is advised to use an average in correlation to the respective field size and depth during calculation.



CHAPTER FIVE

CONCLUSION AND RECOMMENDATION

5.1 CONCLUSION

The studies on the dependence of timer error calculations on field sizes and treatment depth have been done.

The timer error dependence on field sizes showed irregular polynomial of the order of fifth power. The mean values of the absolute timer errors for the various field sizes were found to be as follows: 0.65 s for the $5 \times 5 \text{ cm}^2$ field size, 0.65 s for the $10 \times 10 \text{ cm}^2$ field size, 0.62 s for the $15 \times 15 \text{ cm}^2$ field size, 0.63 s for $20 \times 20 \text{ cm}^2$ field size, 0.64 s for the $30 \times 30 \text{ cm}^2$ field size, and 0.64 s for the $35 \times 35 \text{ cm}^2$ field size.

The teletherapy timer error variations with treatment depths showed irregular polynomial of order fourth power. The mean values were as follows; 0.65 s for the depth of 5 cm, 0.58 s for the depth of 7 cm, 0.61 s for the depth of 10 cm, 0.67 s for the depth of 15 cm, and 0.62 s for the depth of 20 cm.

Comparing the two set-up techniques used with this work, it was noted that the field size variation and depth variation showed almost similar timer value to the degree of 10^{-1} .

However, the treatment depth variations showed the lowest value as compared to field size variations.

Based on the findings from this experimental work, it can be concluded that teletherapy timer error dependence on field size and treatment depth must be incorporated into the

treatment planning calculations for patients undergoing radiotherapy in order to minimize errors due to inaccurate timer error estimation in dose delivery at the NCRNM of the KBTH.

5.2 RECOMMENDATION

Below are the recommendations made as a result of the findings of this experimental work to various stake holders in the treatment of cancer at the NCRNM of Korle Bu, Clinical Community, Policy Makers and Regulators and the Research Community.

5.2.1 Clinical Community

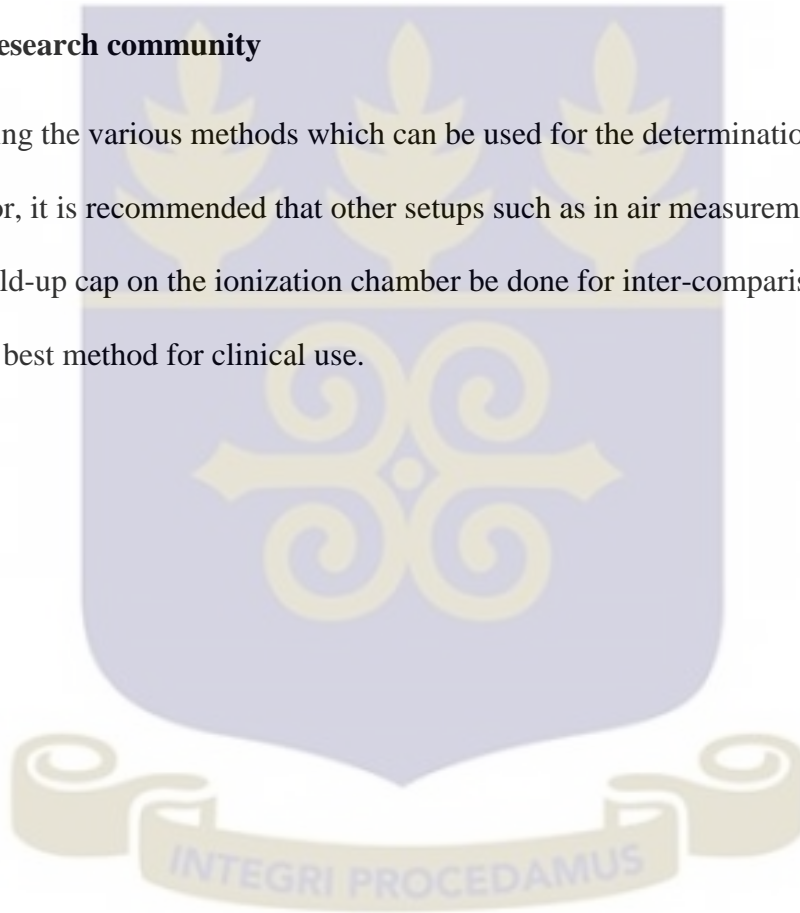
Because not much work has been done on the effects of timer error on both field size and treatment depth, most centers ignore these effects of the field size and treatment depth. It is recommended that a calculation table for the variations of depth and field size with respect to teletherapy timer error be created for monitor unit calculations done by the physicist. This table can be created similar to TPR or TMR tables used for timer value calculations. Monthly evaluation of timer error value by the NCRNM should be done to help provide an efficient and accurate dosimetry for patient treatment.

5.2.2 Policy Makers and Regulators

It is recommended that Policy makers and the Nuclear Regulatory Authority of Ghana make sure that all radiotherapy centers develop treatment protocols that take into account the dependence of field size and treatment depth on teletherapy timer error calculations.

5.2.3 Research community

Considering the various methods which can be used for the determination of teletherapy timer error, it is recommended that other setups such as in air measurements with the use of the build-up cap on the ionization chamber be done for inter-comparison purposes to adopt the best method for clinical use.



REFERENCES

- [1] Breneman J., MD and Warrick R., MD, (2003),” Introduction to Radiation therapy”. Precision Radiotherapy.
- [2] Physician Characteristics and Distribution in the U.S., 2010 Edition, 2004 IMV Medical Information Division, 2003 SROA Benchmarking Survey.
- [3] Professor Vicker S., (2007) Dosimetry: RDTH3120.
- [4] Rontgen W.C., (1895),”Uber eine neue Art von Strahlen. Vorl” aufige Mitteilung. In: Sitzungsberichte” der physikalisch-medicinischen Gesellschaft zu Wurzburg, Sitzung 30, 132–141
- [5] Lederman M., (1981), “The early history of radiotherapy: 1895–1939”, Int. J. Radiat. Oncol. Biol. Phys. 7, 639–648
- [6] Singh AD, Pelayes DE, Seregard S, Macklis R (eds), (2013)”Ophthalmic Radiation Therapy. Techniques and Applications”, Dev Ophthalmol. Basel, Karger, vol 52, pp 1–14 (DOI: 10.1159/000351045)
- [7] Canadian Cancer Society, (2005),” Radiation Therapy: A Guide for People with Cancer”, Toronto, ON: Canadian Cancer Society.
- [8] Haas ML., Varricchio, C., Pierce, M., Hinds, P.S., & Ades, T. B., (2004),” Cancer Source Book for Nurses. (8th Edition)”, Sudbury, MA: Jones and Bartlett Publishers. 8 :pp 131-147

- [9] International Atomic Energy Agency, (1987),” Absorbed dose determination in photon and electron beams: An international code of practice”, IAEA Technical Report Series no. 277, Vienna, Austria
- [10] International Atomic Energy Agency, (1997),” Absorbed dose determination in photon and electron beams: An international code of practice”, IAEA Technical Report Series no. 277 (2nd Edition), Vienna, Austria.
- [11] International Atomic Energy Agency, (2000),” Absorbed dose determination in external beam radiotherapy: An international code of practice for dosimetry based on standards of absorbed dose to water”, IAEA Technical Report Series no. 398, Vienna, Austria.
- [12] Orton C. G. and Seibert J. B., (1972) Phys. Med. Biol., 17,198-205
- [13] Rozenfeld M. L., Phys. Med. Biol., 17, 861-863 (1972).
- [14] Mayles P., Nahum A., and Rosenwald J. C., (2007), “Handbook of Radiotherapy Physics: Theory and Practice”, Published by Taylor and Francis Group, LLC; Vol. 12: 225-244
- [15] Cohen M. and Mitchell J. S., (1984)”, Cobalt-60 Teletherapy: A Compendium of International Practice”, International Atomic Energy Agency, Vienna
- [16] National Council on Radiation Protection and Measurements, (1981),”Dosimetry of x-ray and gamma-ray beams for radiation therapy in the energy range 10 keV to 50 MeV”, NCRP report No.69, Washington DC.

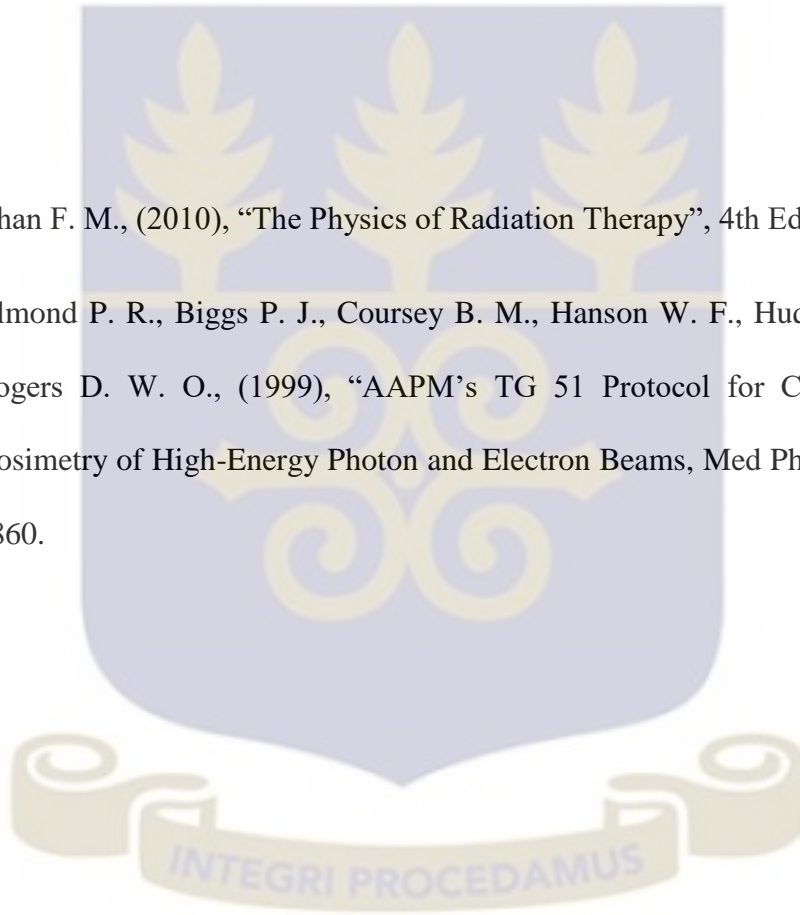
- [17] Stanton R. and Stinson D., (1996), "Applied Physics for Radiation Oncology", Medical Physics Publishing, Madison, Wisconsin.
- [18] Massey J. B., (1970) "Manual of Dosimetry in Radiotherapy IAEA-TRS No.110", International Atomic Energy Agency, Austria, Vienna.
- [19] Bomford C.K., Kunkler I.H. and Sherriff S.B.,(1993),"Textbook of Radiotherapy: Radiation Physics, Therapy and Oncology", Churchill Livingstone, London.
- [20] Mayles P., Nahum A., and Rosenwald J. C., (2007), "Handbook of Radiotherapy Physics: Theory and Practice", Published by Taylor and Francis Group, LLC; Vol. 12: 225-244.
- [21] E.B. PODGORSK, (2005)," TREATMENT MACHINES FOR EXTERNAL BEAM RADIOTHERAPY" Department of Medical Physics, McGill University Health Centre, Montreal, Quebec, Canada pp. 130-135.
- [22] Piet-Hein van der Giessen, Jose Alert et. al., (2004), "Multinational assessment of some operational costs of teletherapy. Radiotherapy and Oncology", vol.71, pp.347-355.
- [23] Li J. S., Pawlicki T., Deng J., Jiang S. B. and Ma C. M., (2002), "Simulation of Beam Modifiers for Monte Carlo Treatment. Radiation Oncology Department", Stanford University School of Medicine. Stanford, CA 94305, USA
- [24] Prof. Sharma S. C., (2007) "Beam modification devices in Radiotherapy", Department of Radiotherapy, PGIMER. Pub, 10

- [25] Garant, Leuven, (1997), "Monitor unit calculation for high energy photon beams", ESTRO EUROPEAN SOCIETY FOR THERAPEUTIC RADIOLOGY AND ONCOLOGY, IAEA INTERNATIONAL ATOMIC ENERGY AGENCY ESTRO Booklet no. 3 (Physics for Clinical Radiotherapy),
- [26] Arthur, Boyer, Ph.D., Peter Biggs, Ph.D., James Galvin, D.Sc., Eric Klein, M.Sc., Thomas LoSasso, Ph.D., Daniel Low, Ph.D., Katherine Mah, M.Sc., Cedric Yu, D.Sc., (2001), " AAPM REPORT NO. 72, BASIC APPLICATIONS OF MULTILEAF COLLIMATORS", Report of Task Group No. 50
- [27] Matjaž Jeraj, Vlado Robar, (2001)" Multileaf collimator in radiotherapy", Radiation Therapy Committee, Department of Radiotherapy, Institute of Oncology, Ljubljana, Slovenia.
- [28] International Atomic Energy Agency, (2001), "Absorbed Dose Determination in External Beam Radiotherapy", Technical Report Series No. 398. Vienna,.
- [29] Samat S. B., Evans C. J., Kadni T. and Dolah M. T., (2008) "The determination of timer error and its role in the administration of specified doses", Jurnal fizik Malaysia, Volume 29, number 1 & 2.
- [30] Orton, C.G., Seibert, J.B., (1972)," The measurement of teletherapy unit timer errors", Phys. Med. Biol. 17 198-205.
- [31] Mayles P., Nahum A., and Rosenwald J. C., (2007), "Handbook of Radiotherapy Physics: Theory and Practice", Published by Taylor and Francis Group, LLC; Vol. 12: 225-244.

- [32] Poffenbarger B. A. and Podgorsak E. B., (1998), “Viability of an isocentric cobalt 60 teletherapy unit for stereotactic radiosurgery”, *Med. Phys.*, Vol. 25; 1935–1943.
- [33] Indra J Das, Chee-Wai Cheng, Ronald J.Watts, Andres Ahnesjo, John Gibbons, X. Allen Li, Jessica Lowenstein, Raj K. Mitra, William E. Simon, Timothy C. Zhu., (2008),” Accelerator beam data commissioning equipment and procedures: Report of the TG-106 of the Therapy Physics Committee of the AAPM”. DOI: 10.1118/1.2969070
- [34] Ervin B. Podgorssak, (2003),“ Review of Radiation Oncology Physics: A Handbook for Teachers and Students”. Department of Medical Physics, McGill University Health Centre, Montréal, Québec, Canada, Chapter 6.
- [35] J. J. M. van Gasteren, S. Heukelom, H. N. Jager, B. J. Mijnheer, R. van der Laarse, H. J. van Kleffens, J. L. M. Venselaar, C. F. Westermann, (1997), “Determination and use of scatter correction factors of megavoltage photon beams”. Report 12 of the Netherland Commission on Radiation Dosimetry.
- [36] Warrington, A. P. and Adams, E. J., (2001),” Conformal and intensity modulated radiotherapy using cobalt-60 and 6 MV x-ray beams: A treatment planning comparison of different sites”, *Radiotherapy Oncology*, vol. 61; (Suppl. 1); S73–S74.

- [37] Khan F. M., (2010), “The Physics of Radiation Therapy”, 4th Edition; 235-245.
- [38] Almond P. R., Biggs P. J., Coursey B. M., Hanson W. F., Huq M. S., Math R., Rogers D. W. O., (1999), “AAPM’s TG 51 Protocol for Clinical Reference Dosimetry of High-Energy Photon and Electron Beams, Med Phys. 26 (9); 1848 - 1860.

37. Khan F. M., (2010), “The Physics of Radiation Therapy”, 4th Edition; 235-245.
38. Almond P. R., Biggs P. J., Coursey B. M., Hanson W. F., Huq M. S., Math R., Rogers D. W. O., (1999), “AAPM’s TG 51 Protocol for Clinical Reference Dosimetry of High-Energy Photon and Electron Beams, Med Phys. 26 (9); 1848 - 1860.



APPENDICES

**APPENDIX A Raw data measurements showing the mean corrected
electrometer readings, temperatures during readings and
pressure reading for variations in field sizes.**

APPENDIX A1 Field size of $5 \times 5 \text{ cm}^2$

FIELD SIZE = $5 \times 5 \text{ [cm]}^2$							
TIMER	ELECTROMETER READINGS		MEAN	MEAN CORRECTED READINGS/nC	Ti/°c	Tf/°c	Pressure/Pa
30.0	9.100	9.088	9.094	9.085	22.7	22.7	1012.5
60.0	18.010	18.000	18.005	17.987	22.7	22.7	
90.0	26.920	26.910	26.915	26.888	22.7	22.7	
120.0	35.840	35.820	35.83	35.794	22.7	22.7	
150.0	44.730	44.720	44.725	44.680	22.7	22.7	
180.0	53.630	53.610	53.62	53.566	22.7	22.7	

APPENDIX A2 Field size of $10 \times 10 \text{ cm}^2$

FIELD SIZE = $10 \times 10 \text{ [cm]}^2$							
TIMER	ELECTROMETER READINGS		MEAN	MEAN CORRECTED READINGS/nC	Ti/°c	Tf/°c	Pressure/Pa
30.0	10.030	10.030	10.03	10.020	22.7	22.7	1012.5
60.0	19.860	19.850	19.855	19.835	22.7	22.7	
90.0	29.680	29.680	29.68	29.650	22.7	22.7	
120.0	39.510	39.500	39.505	39.465	22.7	22.7	
150.0	49.310	49.320	49.315	49.266	22.7	22.7	
180.0	59.150	59.130	59.14	59.081	22.7	22.7	

APPENDIX A3 Field size of $15 \times 15 \text{ cm}^2$

FIELD SIZE = $15 \times 15 \text{ [cm]}^2$							
TIMER	ELECTROMETER READINGS		MEAN	MEAN CORRECTED READINGS/nC	Ti/°c	Tf/°c	Pressure/Pa
30.0	10.640	10.640	10.64	10.629	22.7	22.7	1012.5
60.0	21.060	21.060	21.06	21.039	22.7	22.7	
90.0	31.480	31.470	31.475	31.444	22.7	22.7	
120.0	41.900	41.910	41.905	41.863	22.7	22.7	
150.0	52.330	52.330	52.33	52.278	22.7	22.7	
180.0	62.740	62.750	62.745	62.682	22.7	22.7	

APPENDIX A4 Field size of $20 \times 20 \text{ cm}^2$

FIELD SIZE = $20 \times 20 \text{ [cm]}^2$							
TIMER	ELECTROMETER READINGS		MEAN	MEAN CORRECTED READINGS/nC	Ti/°c	Tf/°c	Pressure/Pa
30.0	11.090	11.080	11.085	11.074	22.7	22.7	1012.5
60.0	21.950	21.950	21.95	21.928	22.7	22.7	
90.0	32.810	32.800	32.805	32.772	22.7	22.7	
120.0	43.660	43.670	43.665	43.621	22.7	22.7	
150.0	54.520	54.530	54.525	54.470	22.7	22.7	
180.0	65.370	65.390	65.38	65.315	22.7	22.7	

APPENDIX A5 Field size of $30 \times 30 \text{ cm}^2$

FIELD SIZE = $30 \times 30 \text{ [cm]}^2$							
TIMER	ELECTROMETER READINGS		MEAN	MEAN CORRECTED READINGS/nC	Ti/°c	Tf/°c	Pressure/Pa
30.0	11.650	11.640	11.645	11.633	22.7	22.7	1012.5
60.0	23.050	23.060	23.055	23.032	22.7	22.7	
90.0	34.450	34.440	34.445	34.411	22.7	22.7	
120.0	45.850	45.850	45.85	45.804	22.7	22.7	
150.0	57.260	57.260	57.26	57.203	22.7	22.7	
180.0	68.660	68.660	68.66	68.591	22.7	22.7	

APPENDIX A6 Field size of $35 \times 35 \text{ cm}^2$

FIELD SIZE = $35 \times 35 \text{ [cm]}^2$							
TIMER	ELECTROMETER READINGS		MEAN	MEAN CORRECTED READINGS/nC	Ti/°c	Tf/°c	Pressure/Pa
30.0	11.790	11.790	11.79	11.778	22.7	22.7	1012.5
60.0	23.330	23.330	23.33	23.307	22.7	22.7	
90.0	34.860	34.870	34.865	34.830	22.7	22.7	
120.0	46.410	46.410	46.41	46.364	22.7	22.7	
150.0	57.960	57.960	57.96	57.902	22.7	22.7	
180.0	69.490	69.490	69.49	69.421	22.7	22.7	



APPENDIX B Raw data measurements showing the mean corrected electrometer readings, temperatures during readings and pressure reading for variations in depth.

APPENDIX B1 Depth of 5cm

DEPTH = 5cm							
TIMER	ELECTROMETER READINGS		MEAN	MEAN CORRECTED READINGS/nC	Ti/°c	Tf/°c	Pressure/Pa
30.0	10.030	10.030	10.03	10.020	22.7	22.7	1012.5
60.0	19.860	19.850	19.855	19.835	22.7	22.7	
90.0	29.680	29.680	29.68	29.650	22.7	22.7	
120.0	39.510	39.500	39.505	39.465	22.7	22.7	
150.0	49.310	49.320	49.315	49.266	22.7	22.7	
180.0	59.150	59.130	59.14	59.081	22.7	22.7	



APPENDIX B2 Depth of 7cm

DEPTH = 7cm							
TIMER	ELECTROMETER		MEAN	MEAN CORRECTED	Ti/°c	Tf/°c	Pressure/Pa
	READINGS						
30.0	8.827	8.827	8.827	8.818	22.7	22.7	1012.5
60.0	17.480	17.480	17.48	17.463	22.7	22.7	
90.0	26.140	26.130	26.135	26.109	22.7	22.7	
120.0	34.790	34.790	34.79	34.755	22.7	22.7	
150.0	43.440	43.440	43.44	43.397	22.7	22.7	
180.0	52.110	52.110	52.11	52.058	22.7	22.7	

APPENDIX B3 Depth of 10cm

DEPTH = 10cm							
TIMER	ELECTROMETER		MEAN	MEAN CORRECTED	Ti/°c	Tf/°c	Pressure/Pa
	READINGS						
30.0	7.205	7.213	7.209	7.202	22.7	22.7	1012.5
60.0	14.280	14.270	14.275	14.261	22.7	22.7	
90.0	21.340	21.340	21.34	21.319	22.7	22.7	
120.0	28.410	28.410	28.41	28.382	22.7	22.7	
150.0	35.480	35.470	35.475	35.440	22.7	22.7	
180.0	42.530	42.540	42.535	42.492	22.7	22.7	

APPENDIX B4 Depth of 15cm

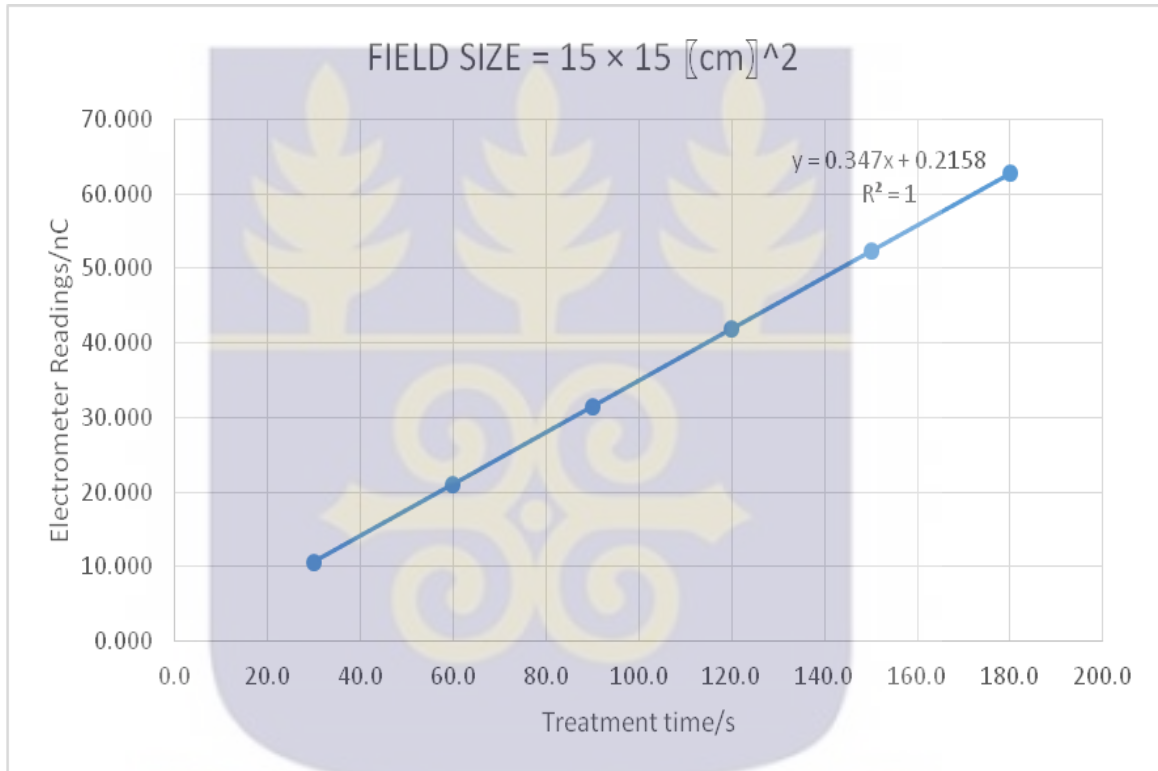
DEPTH = 15cm							
TIMER	ELECTROMETER		MEAN	MEAN CORRECTED	Ti/°c	Tf/°c	Pressure/Pa
	READINGS						
30.0	5.032	5.036	5.034	5.029	22.7	22.7	1012.5
60.0	9.962	9.959	9.9605	9.951	22.7	22.7	
90.0	14.890	14.890	14.89	14.875	22.7	22.7	
120.0	19.810	19.810	19.81	19.790	22.7	22.7	
150.0	24.740	24.730	24.735	24.710	22.7	22.7	
180.0	29.660	29.670	29.665	29.635	22.7	22.7	

APPENDIX B5 Depth of 20cm

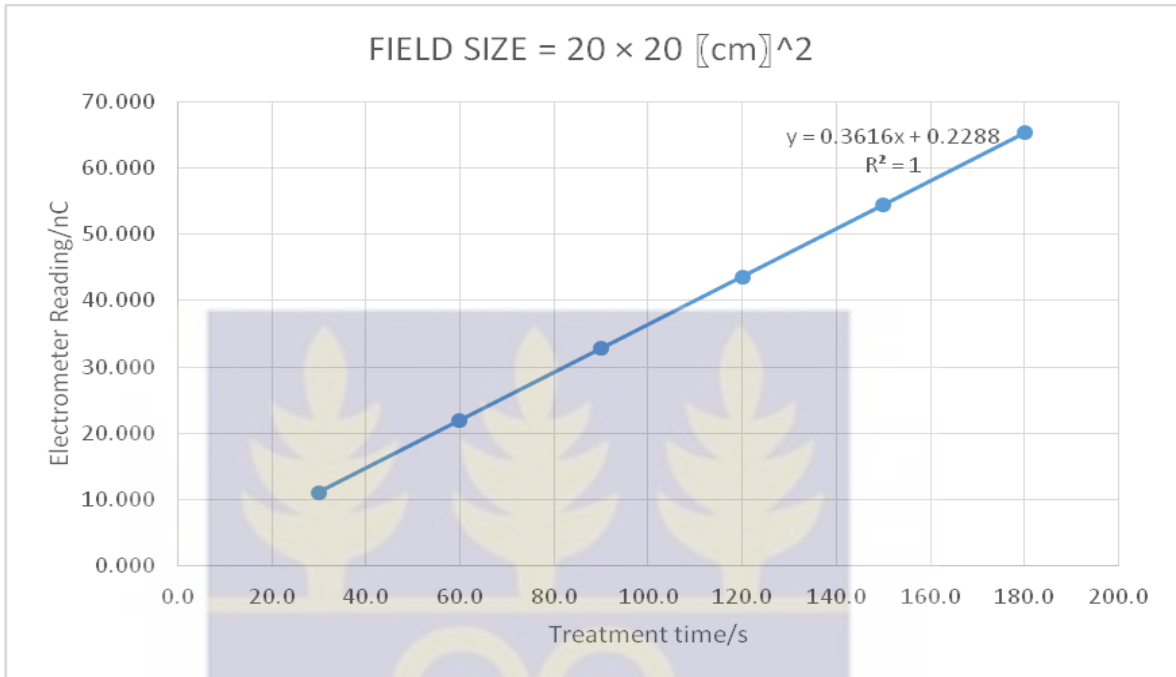
DEPTH = 20cm							
TIMER	ELECTROMETER		MEAN	MEAN CORRECTED	Ti/°c	Tf/°c	Pressure/Pa
	READINGS						
30.0	3.471	3.474	3.4725	3.469	22.7	22.7	1012.5
60.0	6.877	6.875	6.876	6.869	22.7	22.7	
90.0	10.280	10.270	10.275	10.265	22.7	22.7	
120.0	13.670	13.680	13.675	13.661	22.7	22.7	
150.0	17.070	17.080	17.075	17.058	22.7	22.7	
180.0	20.480	20.490	20.485	20.465	22.7	22.7	

APPENDIX C Plotted graphs of corrected readings against treatment time for variations in field sizes.

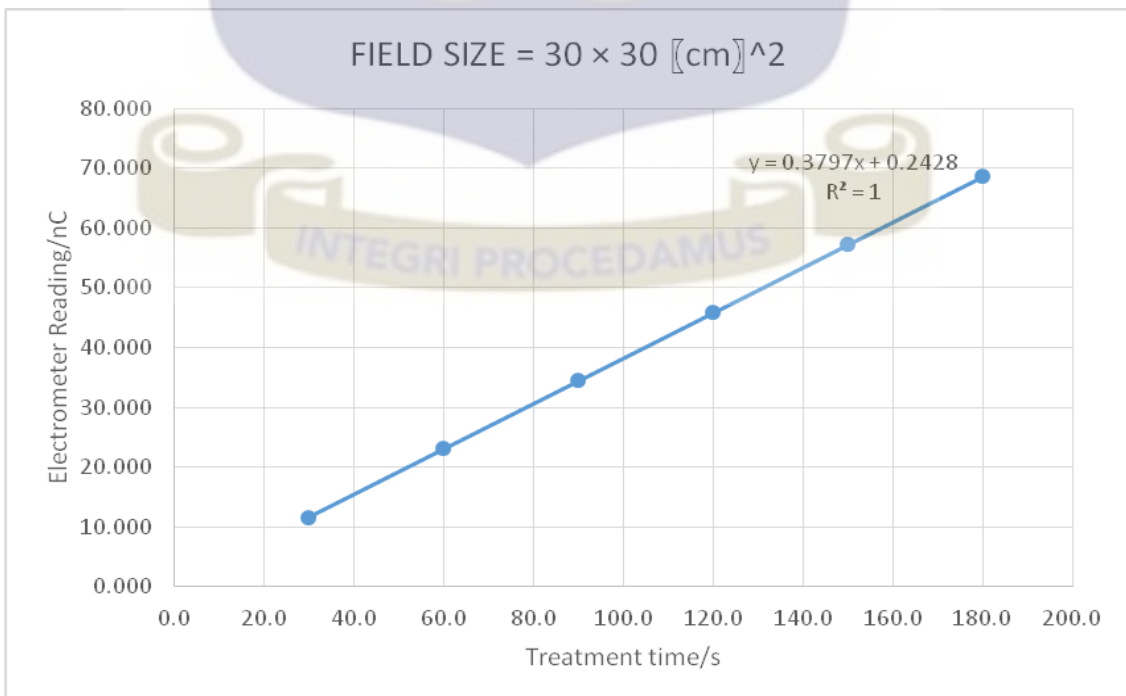
APPENDIX C1 Field size of $15 \times 15 \text{ cm}^2$



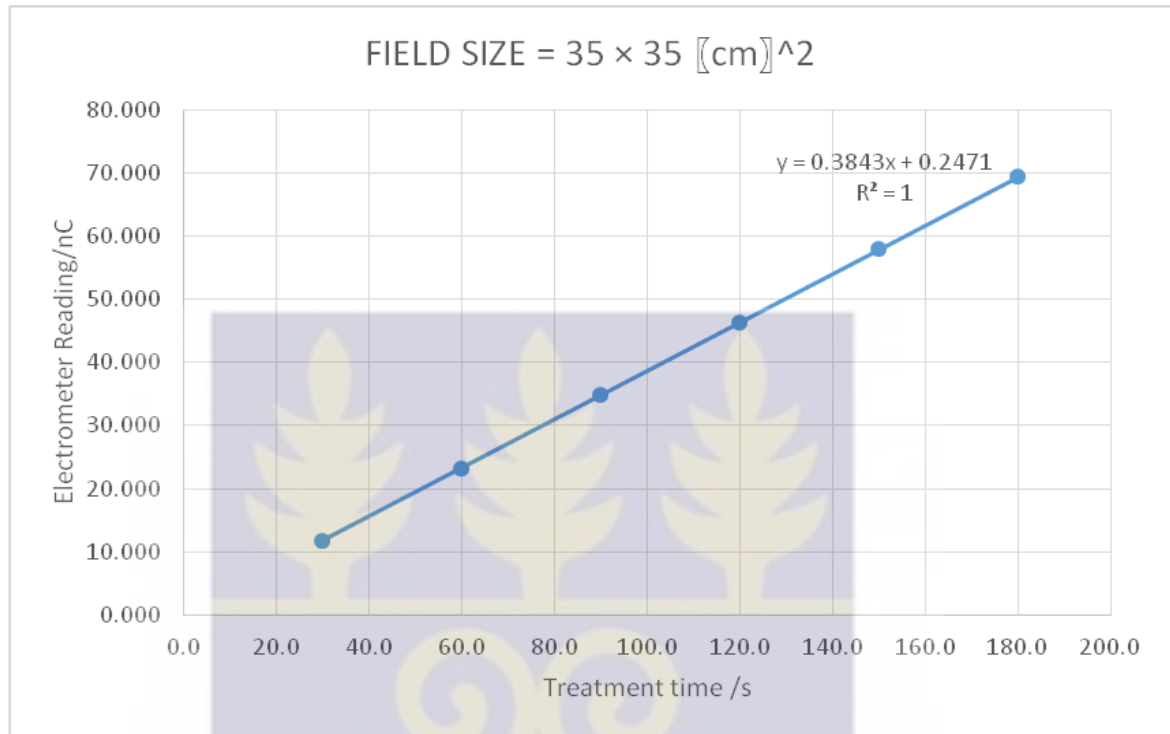
APPENDIX C2 **Field size of $20 \times 20 \text{ cm}^2$**



APPENDIX C3 **Field size of $30 \times 30 \text{ cm}^2$**

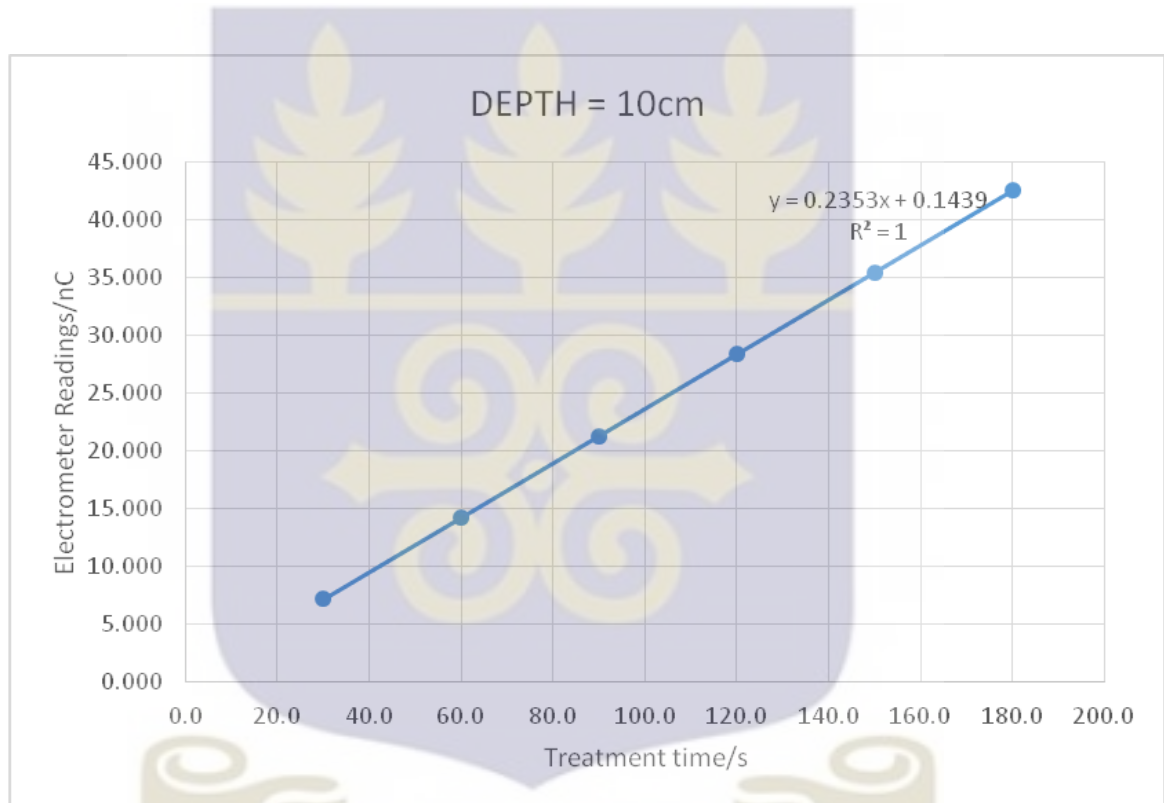


APPENDIX C4 Field size of 35×35 cm²

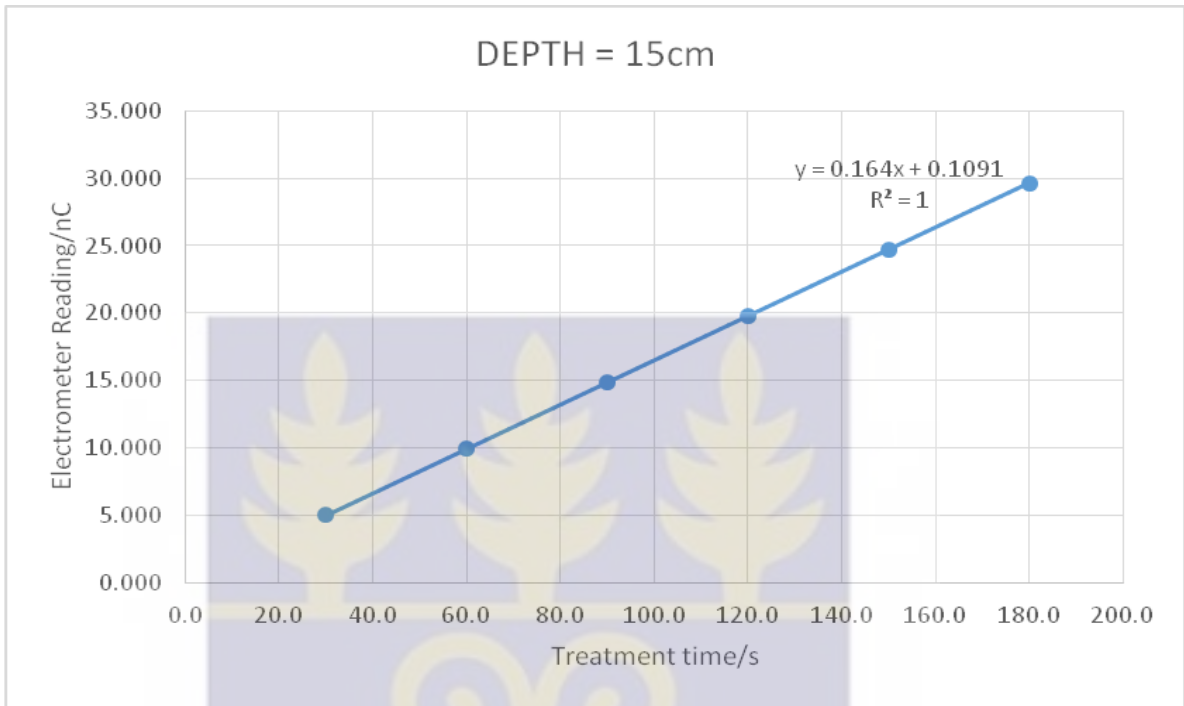


APPENDIX D **Plotted graphs of corrected readings against treatment time for variations in depths.**

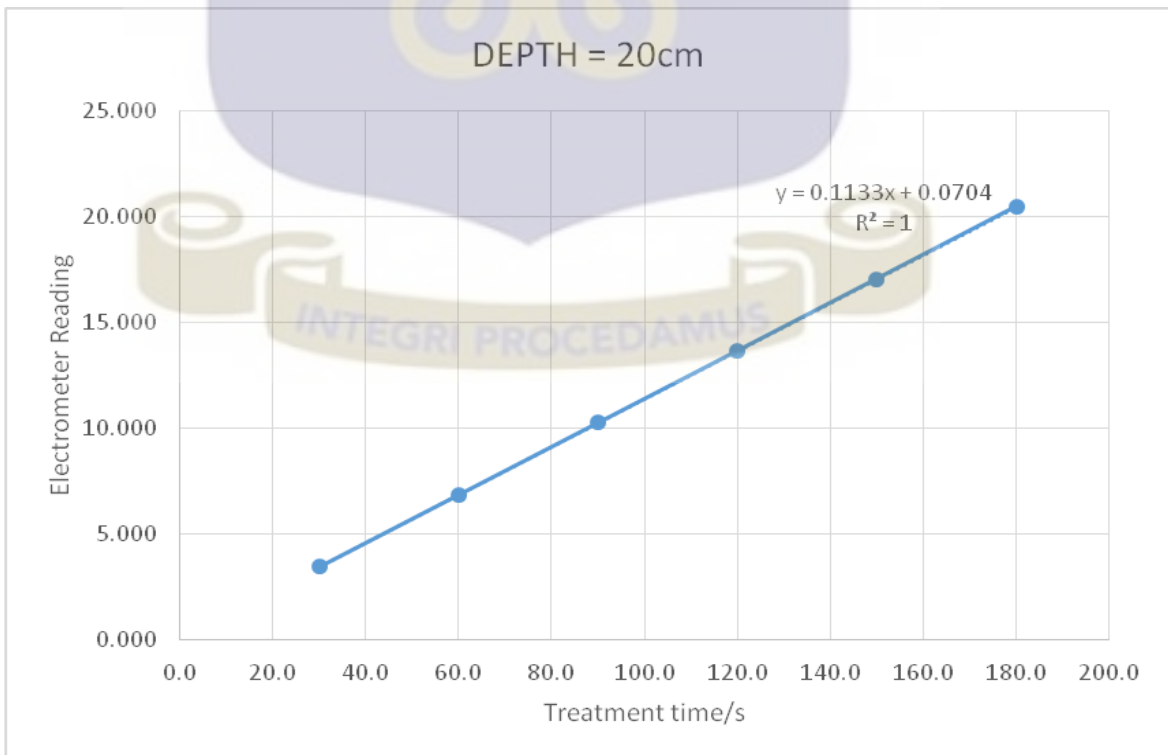
APPENDIX D1 **Depth of 10cm**



APPENDIX D2 Depth of 15cm



APPENDIX D3 Depth of 20cm



**APPENDIX E1 Calculation table for timer error with variation to field size
and treatment depth**

		ONE SIDE OF A SQUARE FIELD					
		5	10	15	20	30	35
Depth	5	0.65	0.65	0.62	0.63	0.64	0.64
	7	0.62	0.58	0.60	0.61	0.61	0.61
	10	0.63	0.61	0.62	0.62	0.63	0.63
	12	0.66	0.66	0.64	0.65	0.65	0.65
	15	0.66	0.67	0.64	0.65	0.65	0.65
	17	0.65	0.65	0.63	0.64	0.64	0.65
	20	0.64	0.62	0.62	0.63	0.63	0.63
	22	0.61	0.57	0.60	0.60	0.60	0.61
	25	0.69	0.72	0.67	0.68	0.68	0.68

